HHS Public Access

Author manuscript

Cell Microbiol. Author manuscript; available in PMC 2020 March 01.

Published in final edited form as:

Cell Microbiol. 2019 March ; 21(3): e12976. doi:10.1111/cmi.12976.

Host membrane glycosphingolipids and lipid microdomains facilitate *Histoplasma capsulatum* internalization by macrophages.

Allan J. Guimarães[1,2,§], **Mariana Duarte de Cerqueira**[3,§], **Daniel Zamith-Miranda**[3,§], **Pablo H. Lopez**[4,#], **Marcio L. Rodrigues**[3,5], **Bruno Pontes**[6], **Nathan B. Viana**[6,7], **Carlos M DeLeon-Rodriguez**[8], **Diego Conrado Pereira Rossi**[8], **Arturo Casadevall**[8], **Andre M.O. Gomes**[9], **Luis R. Martinez**[10], **Ronald L. Schnaar**[4], **Joshua D. Nosanchuk**[2], **Leonardo Nimrichter**[3]

[1]Department of Microbiology and Parasitology, Biomedical Institute, Fluminense Federal University, RJ, Brazil

[2]Departments of Medicine (Division of Infectious Diseases) and Microbiology and Immunology, Albert Einstein College of Medicine, Bronx, NY, USA

[3]Department of General Microbiology, Microbiology Institute, Federal University of Rio de Janeiro, Brazil

[4]Department of Pharmacology and Molecular Sciences, Johns Hopkins University School of Medicine, Baltimore, MD 21205, USA

[5]Instituto Carlos Chagas, Fundação Oswaldo Cruz – Fiocruz, Brazil.

[6]LPO-COPEA, Instituto de Ciências Biomédicas, Universidade Federal do Rio de Janeiro, Brazil.

[7]Instituto de Física, Universidade Federal do Rio de Janeiro, Brazil

[8]Department of Molecular Microbiology and Immunology, Johns Hopkins Bloomberg School of Public Health, Baltimore, MD, USA.

[9]Programa de Biologia Estrutural, Instituto de Bioquímica Médica Leopoldo DeMeis and Instituto Nacional de Ciência e Tecnologia de Biologia Estrutural e Bioimagem, Universidade Federal do Rio de Janeiro, Rio de Janeiro, RJ 21941-902, Brazil.

[10]The University of Texas at El Paso, Biological Sciences, El Paso, Texas, USA

SUMMARY

Recognition and internalization of intracellular pathogens by host cells is a multifactorial process, involving both stable and transient interactions. The plasticity of the host cell plasma membrane is fundamental in this infectious process. Here, the participation of macrophage lipid microdomains

To whom correspondence should be addressed: Leonardo Nimrichter, Instituto de Microbiologia Professor Paulo de Góes, Universidade Federal do Rio de Janeiro, Centro de Ciências da Saude (CCS), bloco I. 21941590, RJ, Brazil. Phone: 55 21 2562 6740. Fax: 55 21 2560 8344, nimrichter@micro.ufrj.br (LN) and Joshua D. Nosanchuk, Albert Einstein College of Medicine, 1300 Morris Park Ave., Bronx, NY 10461, josh.nosanchuk@einstein.yu.edu.

[#]Current Address: Instituto de Investigación Médica Mercedes y Martin Ferreyra (INIMEC–CONICET) and Facultad de Psicología, Universidad Nacional de Córdoba, Córdoba, 5000, Argentina.

[§]AJG and MDC share first authorship on the manuscript.

[*]LN and JDN share senior authorship on the manuscript.

during adhesion and internalization of the fungal pathogen *Histoplasma capsulatum* (Hc) was investigated. An increase in membrane lateral organization, which is characteristic of lipid microdomains, was observed during the first steps of Hc-macrophage interaction. Cholesterol enrichment in macrophage membranes around Hc contact regions and reduced levels of Hc-macrophage association after cholesterol removal also suggested the participation of lipid microdomains during Hc-macrophage interaction. Using optical tweezers (OT) to study cell-to-cell interactions, we showed that cholesterol depletion increased the time required for Hc adhesion. Additionally, fungal internalization was significantly reduced under these conditions. Moreover, macrophages treated with the ceramide-glucosyltransferase inhibitor (P4r) and macrophages with altered ganglioside synthesis (from *B4galnt1* (−/−) mice) showed a deficient ability to interact with Hc. Co-incubation of oligo-GM1 and treatment with Cholera toxin subunit B, which recognizes the ganglioside GM1, also reduced Hc association. Although purified GM1 did not alter Hc binding, treatment with P4 significantly increased the time required for Hc binding to macrophages. The content of CD18 was displaced from lipid microdomains in *B4galnt1* (−/−) macrophages. In addition, macrophages with reduced CD18 expression ($CD18^{low}$) were associated with Hc at levels similar to wild type cells. Finally, CD11b and CD18 co-localized with GM1 during Hc-macrophage interaction. Our results indicate that lipid rafts and particularly complex gangliosides that reside in lipid rafts stabilize Hc-macrophage adhesion and mediate efficient internalization during histoplasmosis.

Keywords

Histoplasma capsulatum; macrophages; lipid rafts; glycosphingolipids

INTRODUCTION

Glycosphingolipids (GSL) are components of plasma membranes of virtually all eukaryotic cells (Hakomori, 2003). Besides their complex roles as components of biological membranes, they also participate in immunoregulatory processes, including modulation of cytokine production and lymphoproliferative responses (Das *et al.*, 2008, Vieira *et al.*, 2008). In concert with sterols, GSL laterally associate with other molecules including pathogen receptors and GPI-anchored proteins within special regions of membranes called lipid microdomains (Brown *et al.*, 2000). Association of pathogen receptors with lipid microdomains implies that these regions are involved in host-pathogen interactions (Triantafilou *et al.*, 2002, Grassme *et al.*, 2003, Triantafilou *et al.*, 2003, Cuschieri *et al.*, 2006). In fact, viruses, bacteria, protozoa, fungi and even prions exploit lipid microdomains to invade phagocytic and non-phagocytic host cells (Lafont *et al.*, 2005, Murphy *et al.*, 2006, Goluszko *et al.*, 2008, Maza *et al.*, 2008, Kalischuk *et al.*, 2009).

Histoplasma capsulatum (Hc) is the etiologic agent of histoplasmosis, one of the most common invasive fungal pulmonary diseases (Cano *et al.*, 2001, Pfaller *et al.*, 2010). This organism is a classical intracellular pathogen that replicates within macrophages and suborns the reticuloendothelial system to disseminate (reviewed by (Kauffman, 2009)). The infection is usually asymptomatic in immunocompetent individuals, although several thousand admissions for histoplasmosis occur annually in the USA (Kauffman, 2009). Disseminated

histoplasmosis is more common in immunocompromised patients, especially in individuals with AIDS (Rodrigues *et al.*, 2008, Kauffman, 2009).

He interacts primarily with CR3 at the macrophage (Mφ) surface (Bullock *et al.*, 1987) through a 60 kDa heat shock protein (HSP60) expressed at the fungal cell wall (Long *et al.*, 2003). CD18, the β subunit of the $\alpha_m\beta_2$ integrin CR3, appears to be the site of CR3 to which Hc binds, although antibodies to CD11b also decrease the association levels (Long *et al.*, 2003, Lin *et al.*, 2010). Internalization of non-opsonized fungi occurs via CR3 and typically results in fungal survival inside resident Mφs (Lin *el al.*, Newman, 1999, Strasser *el al.*, 1999, Shi *el al.*, 2008, Lin *el al.*, 2010).

Here we investigated the role of GSL and lipid microdomains during initial steps of interaction between Hc and murine macrophages (Mφs). Two-photon excitation confocal fluorescence microscopy of live cells was used to show in real-time the formation of organized lipid domains at the site of interaction of Hc with the Mφs membranes. We used cellular systems that included cultured or bone-marrow derived Mφs from mice genetically deficient in the synthesis of complex sialylated GSL (including II^3-N-acetylneuraminosylgangliotetraosylceramide or GM1), CD11b and CD18, with the use of sterol- and GSL-specific reagents and an optical tweezers-based experimental model to evaluate fungus-host cell affinity. Using optical tweezers (OT) we estimated the time required for adhesion between Hc and Mφs, with a focus on the participation of lipid microdomain components. Our results demonstrated that depletion of cholesterol interferes with Hc adhesion kinetics and internalization. The participation of CD18 and CD11b during Hc association was also compared using genetically deficient mice. In addition, GSL participated in the initial steps of Mφ interaction and infection by a fungal pathogen. Interfering with microdomain assembly and protein recruitment could potentially affect macrophage responses, with direct impact on disease development or progression.

RESULTS

Hc contact with the Mφ plasma membrane induces formation of lipid microdomains at contact sites.

Lipid microdomains present a characteristic lateral organization that can be accessed by environment-sensitive fluorescent molecules (Sanchez *et al.*, 2007). Using Laurdan fluorescence microscopy, one can obtain a map of the spatial distribution of lipid phases along the cell membranes. In a time-lapse microscopy experiment these maps are representative of the dynamics of formation and localization of lipid domains in the cell membrane. With this approach, we obtained Laurdan General Polarization or GP images during the interaction between Hc and Mφs in real time. Laurdan GP has been measured before to characterize laterally-organized lipid domains in synthetic and cellular membranes including Mφs membranes (Gaus *et al.*, 2003). To investigate if lipid microdomains are involved in Hc binding to the surface of Mφs we incubated these cells with Laurdan, which partitions into the lipid bilayer. Hc-Rhodamine (Hc-Rho) yeasts were added over the Laurdan-loaded Mφs. The interaction was imaged in a two-photon excitation microscope by a time-lapse sequence of images acquired in real-time during contact and internalization of Hc cells by the Mφs. A time-lapse series of 90 images was acquired (1 frame/s). Fig. 1,

panels A, B and C show, respectively, the Laurdan intensity images at 440 nm, 490 nm and Hc fluorescence at frame number 15. Panels D, E and F show merges of channels 1, 2 and 4, at frames 15, 45 and 75 as representatives of initial, middle and advanced stages of the interaction process. Using the intensity images in channels 1 and 2, the Laurdan GP image sequence can be calculated as described in Materials and Methods and changes in lipid organization at the macrophage membrane level can be followed during the interaction process. Panels G, H and I show the respective GP images of frames 15, 45 and 75, merged with the correspondent Hc fluorescence images. The average change in membrane organization as a function of time is plotted in Fig. 1J. The purple line represents changes in average GP values of all Mφs membranes imaged and the average GP values for specific Hc contact sites are plotted in green (Fig. 1J). The interaction time sequence can be divided in three parts of 30s each. The first 30s show that during the first steps of contact of Hc with macrophages, the GP values on the contact area were higher than the Mφs membranes average (Hc-contact areas mean=0.45 SD=0.01; Mφs mean = 0.38, SD = 0.02, $t(40) = -12.9$, $p = 7.67\times10^{-16}$, significantly different). As the process continues the values of the averages become very close. Finally, in the last 30s there is almost no difference between Hc-contact areas and Mφs, with macrophage membranes average showing a slightly higher average GP value (Hc-contact areas mean = 0.41 SD = 0.017; Mφs mean = 0,42, SD = 0.009, $t(38) = 3.91$, $p = 0.0004$, significantly different). Notably, the average GP of macrophages increased during internalization of Hc (mean of first 10 frames = 0.38, SD=0.006; last 10 frames mean = 0.43 and SD = 0.004; $t(16) = -21.6$, $p = 2.88\times10^{-13}$, significantly different) (Fig 1 and more details in Supplementary Table 1).

Disruption of lipid domains with m-β-CD decreases Hc association with Mφs.

Filipin staining of Hc adhered to J774.16 Mφs revealed enrichment of sterols on the adhesion area (Fig. 2A-D), indicating that cholesterol within microdomains could be involved in Hc- Mφs recognition. Treatment of J774.16 Mφs with methyl-β-cyclodextrin (m-β-CD) removes sterols from cell membranes causing lipid microdomain disruption. To test this hypothesis we then measured the percentage of Hc-Mφs association, which includes the total of Mφs where Hc are adhered or internalized, in the presence and absence of m-β-CD. Incubation of Mφs with m-β-CD decreased their association with Hc in a dose dependent fashion (Fig. 2D-E), especially at early time points (15 min, Fig 2D). Although opsonization with a monoclonal antibody (mAb) to heat shock protein 60 (HSP60) (mAb 7B6) did not change the association level in control Mφs, it partially reversed the inhibition caused by previous m-β-CD treatment. A second mAb against a different surface antigen (M antigen, mAb 6F12) had a similar effect (Fig. 2D-E). When the incubation period was increased to 45 min, a similar tendency was observed but no statistical differences were detected (Fig. 2E). Overall, the association of opsonized yeast was abruptly decreased by m-β-CD treatment after 15 min of interaction, with a significant reversion in the magnitude of effect over time suggesting that remodeling of microdomains is important during the initial steps of fungi-phagocyte interaction.

Mφ metabolic integrity was assessed using methylthiazolyldiphenyl-tetrazolium (MTT) 1h after treatment with m-β-CD (0 to 20 mM). At the highest dose, a trend toward lower metabolic activity was observed, as previously described in several models (Piel *et al.*, 2007,

Kainu *et al.*, 2010). However, using a Trypan Blue assay, the cells displayed ~100% of membrane integrity in all conditions tested (data not shown).

Fungal adhesion to Mφs is dependent on the integrity of lipid rafts.

The results above indicate that lipid raft disruption might interfere with the kinetics of Hc-Mφs association. Using optical tweezers (OT) we were able to access this kinetics by measuring the characteristic time (τ) required for adhesion of Hc to Mφs, the step that precedes fungal phagocytosis. A plot of the relative adhesion as a function of time revealed that the number of positive adhesions between Hc and J774.16 Mφs increased with time in all experimental conditions (Fig. 3). Treatment with 10 mM m-*β*-CD slowed the rate of yeast-Mφ stable adhesion nearly 3-fold. Whereas opsonization increased the rate of association to both control and m-*β*-CD-trcatcd Mφs, raft disruption again slowed the relative rate of stable adhesion, in this case ~4-fold. The characteristic time values obtained by optical tweezers are in agreement with the association results.

Treatment with m-β-CD also reduces the capacity of Mφs to phagocytose Hc.

Cholesterol depletion influences adhesion during the first minutes of Mφs-Hc interaction. We then investigated whether treatment with m-*β*-CD also impacts Hc internalization by J774.16 Mφs after 45 minutes interaction (Fig. 4A and Supplementary Table 2). When experiments were performed using non-opsonized fungi and control Mφs, we observed that 71% of associated Hc were internalized in 45 min. For these analyses, only the Mφs containing at least one Hc attached were considered for comparison between adhered and internalized yeasts. Furthermore, since there was no difference between GFP-Hc and NHS-Rho-Hc association to Mφs (data not shown), NHS-Rho did not impair Hc recognition by Mφs. Treatment with 5 and 10 mM m-β-CD reduced the internalization of Hc by treated Mφs by nearly 20%. Treatment with 20 mM m-β-CD resulted in almost complete abrogation of internalization. Inhibition of phagocytosis was overcome by opsonization of yeasts with antibodies to HSP60, except at the highest concentration of m-β-CD, in which the inhibitory conditions was only slightly reduced by opsonization. This observation is in agreement with a possible impairment of interaction through FcγR or an alternative mechanism of association of yeast by a low affinity non-raft receptor. In combination with the observation that only the treatment with 20 mM m-*β*-CD efficiently reduced the association index at 45 min (Fig. 2), these data suggest that cholesterol depletion impacts both adhesion and internalization of Hc by Mφs. Since m-*β*-CD efficiently extracts proteins from cell surfaces (Ilangumaran *et al.*, 1998), we next tested whether CR3 components were normally detected in m-*β*-CD-treated cells. The membrane levels of CD18 and CD11b, which are well-characterized receptors for Hc (Long *et al.*, 2003), were not altered by m-*β*-CD treatment (Figure 4B).

Inhibition of GSL synthesis by Mφs reduces Hc association.

We then explored the role of GSL, another class of lipids enriched in microdomains, during Hc association by using J774.16 Mφs treated with P4 ((1*R*,2*R*) 1-phenyl-2-palmitoylamino-3-pyrrolidino-1-propanol), a specific inhibitor of GSL biosynthesis (Nicholson *et al.*, 1999). Mφs were treated with P4r (active isomer) or P4s (the 1.*S*,2*S* inactive isomer) as a control for three days. Under the conditions used in our experiments

P4r treatment resulted in −60% inhibition of ganglioside synthesis in bone-marrow derived Mφs (Fig. S1). Treatment also minimally reduced sphingomyelin and ceramide (−10 and 14% respectively), when compared with the inactive control P4s (Fig. S2). In addition, P4r treatment reduced the Mφ-Hc association by 30% compared to P4s treated cells ($p<0.05$), suggesting the involvement of gangliosides during Hc infection of Mφs (Fig. 5A). Corroborating with these data the characteristic time (τ) required for adhesion of Hc yeasts was significantly increased in P4r treated Mφs when compared to the inactive isomer (42 ± 4 s vs. 60 ± 5 s, Fig 5B). We believe treatment with P4 does not impact cytoskeleton stability since no changes were observed in F-actin (Fig. S3). The ability of m-β-CD to extract macrophage gangliosides was also investigated (Fig. S4). Although a small reduction was observed (~21% for GM1 and ~25% for GD1a) when compared to P4 treatment the results were significant, suggesting that a decrease in Hc association to macrophages could be also linked to the reduced amount of gangliosides.

Complex gangliosides are required for Hc- Mφ association.

The data indicating the participation of GSL during fungal association with Mφs led us to determine which gangliosides are synthesized by Mφs and explore their role during interaction with Hc. The resolution of polar lipids extracted from J774.16 Mφs by TLC revealed six major resorcinol-positive (sialic acid-containing) bands (Fig. 5C). Based on their migration, the major gangliosides synthesized by Mφs corresponded to GM3, GM1 and GD1a, each migrating as double bands due to variations in their lipid moieties (Ando *et al.*, 1984). Bone marrow-derived Mφs revealed four major resorcinol-positive bands corresponding to GM1 and GD1a (Fig. S1). The presence of GM1 and GD1a was confirmed by immunostaining (data not shown). Considering that Mφ GSL levels influenced Hc interactions, we analyzed the association of yeast with peritoneal Mφs isolated from *B4galnt1* deficient mice and wild type (WT) mice. *B4galnt1*$^{-/-}$ mice lack the *N*-acetylgalactosaminyltransferase required for the synthesis of complex gangliosides, such as GM1 and GD1a. Instead, they accumulate truncated gangliosides, such as GM3 and GD3 (Sheikh *et al.*, 1999). Peritoneal Mφs from B4galnt1$^{-/-}$ mice were significantly impaired in their capacity to bind Hc compared to Mφs from WT mice, showing an almost complete loss of fungal association ($p<0.02$, Fig. 5D). Hc opsonization with anti-HSP60 mAb partially reversed the reduced capacity of *B4galnt1*$^{-/-}$ Mφs to recognize yeasts, as observed for m-β-CD treatment. This data suggest that Mφs lacking complex gangliosides have an impaired capacity to organize the cell surface apparatus required to recognize Hc. Also, only complex gangliosides, GM1 and GD1a appear to be involved with fungal association, since GM3 accumulates in *B4galnt1*$^{-/-}$ mice.

Cholera toxin subunit B and oligo-GM1 inhibit Hc association with Mφs.

Since the absence of complex gangliosides impaired the recognition of Hc yeasts by Mφs we tested whether GM1 and GD1a could be additional receptors for Hc. In fact, GSL have been described as receptors for bacterial toxins, virus, and fungus (Kroken *et al.*, 2011, Ywazaki *et al.*, 2011, Matrosovich *et al.*, 2015, Oda *et al.*, 2015). In order to do that we tested whether the Cholera toxin subnunit B (CtxB), a well-described ligand for GM1, and the lipid-free glycan derived from GM1 (oligo-GM1) would also interfere with Hc infection. Treatment with CtxB, which blocks part of the available GM1 at the J774.16 Mφ surface, significantly

decreased fungal association (Fig. 5E). As observed for *m-β*-CD treatment, opsonization reversed the inhibition effect of CtxB. We also investigated whether the addition of GM1 could impair binding of Hc to J774.16 Mφs using soluble binding inhibition assays with different concentrations of oligo-GM1. Our results demonstrate that 1, 3 and 9 mM oligo-GM1 resulted in a dose dependent reduction of association to 99%, 89% and 81% respectively, relative to control (Fig. 5F; $p<0.05$). Since CtxB can also modulate the architecture and dynamics of microdomains composition and function (Day *et al.*, 2015) and that the percentage of association inhibition using oligo-GM1 was very low, additional experiments to investigate the participation of complex gangliosides as receptors were performed. Overlay assays in ELISA and HPTLC plates, using immobilized gangliosides (Lopez *et al.*, 2006) and incubations with yeasts of Hc were developed. Under our experimental conditions no direct association between any GSL and Hc yeasts was visualized (data not shown). These results suggest that the role of GM1 in Hc adhesion to phagocytes is accessory and probably involves the microdomains architecture and the participation of other plasma membrane components.

Lack of complex gangliosides interferes with CD18 recruitment to lipid microdomains.

Our results indicated that lipid microdomains disruption and complex gangliosides absence impaired efficient association between Hc and Mφs. However, GM1 and GD1a do not appear to be receptors for Hc yeasts. To explore possible mechanisms regulating this phenomenon we investigated the association between complex gangliosides and CD18 recruitment to lipid microdomains using Mφs from WT and *B4galnt1*$^{-/-}$ mice. Integrin CD18 was chosen as a prototype for mechanistic evaluation because of its well-known role on Hc adhesion to Mφ (Bullock *et al.*, 1987, Long *et al.*, 2003). The CD14 receptor was also examined, since this receptor is a GPI-anchored protein expected to be enriched in lipid domains (Schmitz *et al.*, 2002). The amount of CD14 in lipid microdomains fractions is similar in Mφs from both phenotypes (Fig. 6A and B). Thus, this result indicated that a lack of complex gangliosides does not impair lipid microdomains assembly at the cell surface. In contrast, in comparison to Mφs from WT mice, CD18 was significantly decreased in lipid microdomains fractions isolated from *B4galnt1*$^{-/-}$. Larger amounts of CD18 were found in other fractions that do not correspond to lipid microdomains density fractions (Fig. 6A and B). Remarkably, the levels of CD18 in WT and *B4galnt1*$^{-/-}$ macrophages were similar (Figure S5). Thus, these results indicated that complex gangliosides could be important for the correct maintenance of transmembrane proteins within lipid rafts, and disruption of gangliosides could interfere with Hc association.

Association with Hc is reduced in CD11b$^{-/-}$ *Mφs, but not modified in phagocytes with reduced CD18 expression* (CD18^{low}).

CR3 is composed by α and β integrins (CD18 and CD11b, respectively) with well-recognized adhesive properties (Ehlers, 2000). CD18 is a major ligand for HSP60 displayed at the cell wall of Hc (Long *et al.*, 2003). However, participation of other integrins including CD11a and CD11c cannot be ruled out (Newman *et al.*, 1990). According to Lin and colleagues CD18 is a key protein for Hc phagocytosis by Mφs (Lin *et al.*, 2010). The significant decrease of CD18 detection within lipid rafts isolated from Mφs lacking complex gangliosides led us to investigate the requirement of CD18 to Hc adhesion. Initially, we

confirmed the reduced levels of CD18 staining in the $CD18^{low}$ Mφ by Western Blot (Fig. S6). The association index of Hc to $CD18^{low}$ was similar to that observed for WT Mφs (Fig. 7A). These results were confirmed by OT experiments, which showed that the kinetics of Hc binding to the Mφs was identical in both $CD18^{low}$ and WT cells (data not shown). On the other hand, Mφs lacking CD11b showed a 30% decreased capacity to associate with Hc yeasts (Fig 7A). To confirm this observation, we performed additional experiments of fungus-host cell adhesion using OT, comparing CHO cells expressing the same α (CD18) and distinct β integrins (CD11a, CD11b and CD11c, to form respectively the LFA1, CR3 and CR4) and observed that the rate of yeast-Mφ stable adhesion was higher for CHO expressing CD11b integrins in comparison to CHO null or expressing CD11a or CD11c integrins (Fig. S7). Together, these data suggest that CD11b can also impact Hc-Mφs association.

CD11b and CD18 co-localize with GM1 and Hc yeasts during Mφ *infection*.

Given the potential involvement of GSL in receptor recruitment and stabilization of Hc adhesion to Mφs, we mapped GM1, CD18 and CD11b during infection of bone marrow-derived Mφs. We first examined the distribution of GM1 at the cell surface of Mφs. GM1 was distributed over the entire cell surface, with some punctuate staining (Fig. 7B) similar to what has been published (Huang *et al.*, 2015). We then assessed GM1, CD18 and CD11b distribution at the surface of Mφs infected with Hc. Staining with FITC-labeled CtxB was performed at 4 °C to avoid Hc and CtxB internalization and to impair reorganization of GM1 along the Mφ cell surface (Williamson *et al.*, 1975, Kasai *et al.*, 1976, Martin *et al.*, 1976, Dickens *et al.*, 1981). GM1 was again present along the entire Mφ surface, including the yeast binding sites (Fig. 7B). CD11b and CD18 are distributed over the cell surface of Mφ (Huang *et al.*, 2015). After incubation of Hc with Mφ CD11b was found surrounding the yeast cells in a pattern similarly to that observed for GM1. Reactivity to anti-CD18 was also visualized at the interface between Hc and Mφs (Fig. 7B). These results indicate that both integrins are found in lipid domains surrounding yeasts of Hc yeasts, strongly suggesting the involvement of these lipid-enriched compartments during interaction between Mφ and Hc.

DISCUSSION

Lipid microdomains are nanoscale regions in the membrane that are able to compartmentalize lipids and proteins, forming platforms that coalesce and participate during membrane signaling, trafficking and phagocytosis (Kim *et al.*, 2002, Dykstra *et al.*, 2003, Lafont *et al.*, 2005, Barrias *et al.*, 2007). Exploring lipid microdomains dynamics can shed light on new mechanisms or alternatives for blocking infectious processes. Our experiments indicate that these platforms are involved with the initial kinetics of Hc-Mφ association and fungal internalization. Using live cells we showed that Mφs-Hc interaction induces recruitment of laterally organized lipid domains and Mφ membrane organization, first at the site of fungus-phagocyte contact and then along the entire surface of the host cell. As the process continues, the interaction of Hc with Mφs triggers a general change in membrane organization that apparently persists after internalization of the fungus, potentially affecting future events of phagocyte infection. Membrane plasticity would allow recruitment of other

proteins, modulating Mφs-Hc engagement and the host cell response, as suggested in a previous study (Huang *et al.*, 2015).

We hypothesize that global membrane organization at initial times of interaction could be associated with basal sterol levels, a requirement for ideal membrane plasticity (Marsh, 2009). Changes in or obstructions of microdomains components interferes with adhesion and internalization (Riethmuller *et al.*, 2006). For example, sterol-depleted Mφs are not efficient at internalizing mycobacteria (Gatfield *et al.*, 2000). In this setting, mycobacteria remained loosely attached to the sterol-depleted cell membranes, while control Mφs readily internalized the pathogen. In addition, a higher depletion of sterol content also impairs FcR function in Mφs during Hc adhesion suggesting that engagement and phagocytosis through FcγR is at least partially linked with lipid microdomains assembly. In fact, m-β-CD treatment of Chinese hamster ovary (CHO) cells expressing human FcγRIIA impairs binding and phagocytosis of 4.5 μm polystyrene beads covered with IgG (Vieth *et al.*, 2010). Although these cells are not classical phagocytes these results confirm a possible involvement of lipid rafts during internalization through FcγR. In our model, sterol appears to be necessary mostly during the initial events of interaction between Mφs and Hc yeasts probably through a mechanism that involves microdomain rearrangements. For longer periods of interaction other mechanisms may compensate sterol requirement since the relative associations reach 100% even after m-β-CD treatment. In addition, disruption of the lipid microdomains was overcome in the setting of opsonized yeast, especially during the first 15 minutes of interaction, suggesting a more efficient association through FcR. Decreasing in association levels is usually correlated with adhesion impairment, which we also confirmed by OT analysis. However, sterol depletion also appears to influence internalization of Hc by Mφs. Thus, normal concentrations of sterol are required for optimal adhesion and internalization events during Mφs-Hc recognition.

Membrane cholesterol levels are a key factor in determining microdomain stability and organization (Silvius, 2003) and (glyco)sphingolipids (GSL) constitute a second pool in membrane microdomains (Lafont *et al.*, 2005). Although the major effect of m-β-CD is to deplete sterols from cell membranes, our results demonstrated that this treatment also reduced the presence of GSL in a minor but significant level. We then extended our studies investigating the contribution of sialic acid-containing GSL, the so-called gangliosides, during Hc-Mφs association. Inhibition of GlcCer synthesis by P4r, which affects the levels of all downstream GSLs, resulted in an effective decrease in fungal association and adhesion kinetics. Our results showed that major gangliosides synthesized by Mφs include GM3, GM1 and GD1a. Although an increase of sphingomyelin and ceramide was also observed, the changes are minimal and unlikely to influence Hc-Mφs association. To confirm the requirement for complex gangliosides during Mφs-Hc we used Mφs from *B4galnt1*$^{-/-}$ mice, which the synthesis of complex gangliosides, including GM1 and GD1a, is impaired (Sheikh *et al.*, 1999). Key neural functions for complex gangliosides have been suggested using these animals as models (Sheikh *et al.*, 1999, Sun *et al.*, 2004); however, the impact of altered ganglioside synthesis in infectious processes has not been evaluated. Since both association and adhesion kinetics were decreased when *B4galnt1*$^{-/-}$ Mφs were used two possibilities were raised. First, depletion of GSL would disorganize complexes and modify lateral or side-by-side (*cis*-interactions) associations with other membrane molecules within lipid

domains and interfere with functions of proteins such as integrins from Mφs, resulting in a lower association level with yeasts. Second, gangliosides could be co-receptors during initial steps of interaction with apposing cells (*trans*-interactions), as previously suggested for other GSL (Jimenez-Lucho *et al.*, 1990). GSL have been reported as ligands for different pathogens, including fungi (Bergelson *et al.*, 1982, Krivan *et al.*, 1988a, Krivan *et al.*, 1988b, Jimenez-Lucho *et al.*, 1990, Superti *et al.*, 1991). In *P. brasiliensis*, GM1 has been shown to bind to yeast forms and to accumulate at fungal binding sites in alveolar epithelial cells (Ywazaki *et al.*, 2011). Previous data suggested that GM1 is also recruited to sites of Hc association in host cells (Huang *et al.*, 2015), but no function regarding the importance during the association process was determined. GM1 has also been shown to co-localized with CD44 in human brain microvascular endothelial cells (HBMEC) interacting with *Cryptococcus neoformans* (Huang et al., 2012). In addition, Ywazaki suggested that GM3 and GM1, participate during binding and/or infection by *P. brasiliensis* (Ywazaki *et al.*, 2011). Mobility of GM1 has been demonstrated to impact endocytosis of CtxB, a toxin that specifically binds to this GSL (Pang *et al.*, 2004). Furthermore, internalization of *Escherichia coli* by epithelial cells requires GM1 recruitment (Kansau *et al.*, 2004) and internalization of the intracellular pathogen *Legionella* involves a mechanism dependent on GM1 and GPI-anchored proteins (Watarai *et al.*, 2002).

In our model, inhibition of Hc association after exposure of host cells to CtxB might be the result of steric hindrance or lower mobility of GM1 after binding to the toxin, impairing the recruitment of these molecules to lipid microdomains along with other receptors, which consequently would stabilize the Hc-Mφ interactions. The fact that CD14 is normally enriched in lipid microdomains from *B4galnt1*$^{-/-}$ Mφs suggests that such domains are formed in the absence of complex gangliosides. Thus, Mφs-Hc interaction is not only dependent on microdomains formation, but also to a well-coordinated recruitment of specific molecules, such as complex gangliosides, during their assembly. Several receptors on the Mφ surface are able to mediate interaction with Hc, including CD18, Dectin-1, and TLR (Lin *et al.*, 2010). However, Lin et al. (Lin *et al.*, 2010) suggest that only CD18 is involved with Hc adhesion and internalization in the absence of opsonins. Recently, Huang et al (Huang *et al.*, 2015) demonstrated that Dectin-1 and CR3 crosstalk within lipid microdomains, which in part could explain our results. We also showed that CD18 was significantly decreased in lipid microdomains from *B4galnt1*$^{-/-}$ Mφs, which could result in loose association between the Mφ and Hc. In fact, CD18 partially co-localizes with lactosylceramide (LacCer)-enriched lipid microdomains in the plasma membrane of neutrophils during phagocytosis of nonopsonized zymosan (Nakayama *et al.*, 2008). Accordingly, CD18 is recruited to lipid microdomains and the pre-treatment of neutrophils with anti-LacCer, anti-CD11b and lactose interferes with phagocytosis. Our results initially indicate that complex gangliosides could participate during basal CD18 recruitment to lipid microdomains in Mφs. In addition, GM1 and CD18 could cooperatively act during Hc recognition and trigger amplification of CD18 recruitment, resulting in stable adhesion and initiating signaling for fungal internalization. In addition, OT experiments revealed that CD18^{low} Mφs support Hc adhesion as well as WT. These results indicate that low CD18 expression is sufficient for Mφs–Hc binding. Absence of CD11b culminated with decreased but not null Hc recognition by Mφs, suggesting that intact CR3 is not essential, but enhances

the fungal-phagocyte association. Cell wall β-glucan could attach to the CD11b-lectin site located C-terminal to the I-domain of CD11b and induce changes in the integrin conformation with possibly increased ligand affinity (Thornton *et al.*, 1996, O'Brien *et al.*, 2012). Using OT we confirmed that CHO cells expressing the heterodimers LFA-1 (CD11a/CD18) and CR4 (CD11c/CD18) were also able to support Hc binding but required a higher adhesion time (Figure S7).

Our results demonstrate that membrane microdomain composition impacts Hc recognition by Mφs. Furthermore, they are required for efficient internalization, a step necessary to optimal Hc replication and disease development. We observed that GSL (especially GM1) and membrane microdomains are involved with integrin recruitment and potentially with stability of Hc-Mφ interactions. In addition, Hc internalization through membrane microdomains suggests a selective retention of membrane components with potential segregation of other molecules. The lateral association between proteins and GSL could regulate Mφs function during interaction with Hc through integrin control (Paller *et al.*, 1995, Jia *et al.*, 2016). Membrane microdomains and GSL composition could be then associated with the capacity of Hc to regulate internalization, phagosome maturation, and the intracellular fate of fungus. Future studies are under development to determine whether lipid microdomains and specifically GSL could influence histoplasmosis establishment and impact the orchestration of host immune responses.

EXPERIMENTAL PROCEDURES

Fungal strains and mammalian cells culture.

For phagocytic assays we used the Mφ-like cell J774.16, derived from a reticulum cell sarcoma (ATCC TIB 67) as well as primary or derived murine cells. J774.16 cells were cultured in DMEM with 10% heat-inactivated FBS, 10% NCTC-109 medium, nonessential amino acids (1% by volume of 100 x mixture, Invitrogen) and penicillin-streptomycin (1% by volume, Invitrogen). Hc G217B strain was obtained from the ATCC. Yeast cells were grown in Ham's F-12 medium at 37 °C with rotatory shaking as described (Allendoerfer *et al.*, 1997). GFP-expressing strain G217B (GFP-Hc) was a gift from Dr. George S. Deepe (University of Cincinnati College of Medicine) and cultivated under the same conditions. Yeast were washed three times in PBS and counted by hemacytometer. For all experiments, the Mφ:yeast ratio used was 1:5. CHO cell lines stably transfected with LFA-1 (CD18/CD11a), CR1 (CD35), CR3 (CD18/CD11b) or CR4 (CD18/CD11c) were a gift from D.T. Golenbock (University of Massachusetts Medical School, Boston, Massachusetts, USA). CHO cells were cultured in Ham's F-12 medium supplemented with 1.176 g/L sodium bicarbonate and 5% heat-inactivated FBS at 37 °C.

Mice.

Mice with a disrupted gene for GM2/GD2 synthase, *B4galnt1*$^{-/-}$ were generated by Dr. Richard Proia (US National Institutes of Health.), then extensively back-crossed onto a C57BL/6 background as described (Pan *et al.*, 2005). Four- to eight-week-old female C57BL/6 CD11b$^{-/-}$ (strain B6.129S4-Itgam^{tm1Myd}/J) mice were purchased from Jackson Laboratory (Bar Harbor, MA). CD18^{low} (C57BL/6 genetic background) mice were donated

by Prof. Lucia H. Faccioli (Universidade de Sao Paulo, Brazil). Wild type C57BL/6 mice used as control were purchased from Charles River. Animal procedures were approved by Albert Einstein College of Medicine Animal Care and Use Committees.

Bone marrow-derived (BMDM) and peritoneal Mφs (pMφ).

To prepare pMφ, peritoneal cells were harvested from WT or KO mice using classic protocols (Fortier *et al.*, 2001). Bone marrow cells were differentiated *in vitro* in the presence of RPMI with 10% FBS and 20% L929 supernatant. After 4 days the differentiation media was replaced by new one, and at the 7th day, macrophages were differentiated as confirmed by flow cytometry as F4/80^{+} / LY-6C^{-} cells.

Laurdan confocal fluorescence microscopy and general polarization (GP) measurements.

To investigate the formation of lipid microdomains at the sites of interaction between Hc and Mφs, Laurdan fluorescence spectroscopy combined with spatial resolution optical microscopy were used (Sanchez *et al.*, 2007). Laurdan is a fluorescent probe that intercalates at the membrane perpendicular to the lipid bilayer and distributes equally, independent of the lipid composition of the membrane. Laurdan fluorescence spectrum shifts according to the polarity of the environment (Weber *et al.*, 1979, Parasassi *et al.*, 1990). The spectral change is related to the accessibility of water in the membrane, and thus to the lateral strength of the interactions between lipid chains, representing different lipid phases. This spectral change can be quantified by calculating the ratio between two different emission wavelengths. This value is called the general polarization or GP (Parasassi *et al.*, 1990). The GP theoretical values range from −1 to 1 but for biological membranes, it is known that GP values higher than 0.5 are characteristic of gel phase, values from 0.3 to 0.5 represent liquid organized membranes, which are characteristic of lipid microdomains, and GP values below 0.3 are presented by liquid disordered membrane domains (Parasassi *et al.*, 1990, Sanchez, 2007).

Bone marrow-derived Mφs were plated in glass bottom dishes (MatTek) and incubated in medium containing 20 mM Laurdan for 10 min prior to the addition of Hc-Rho cells (see details below). Laurdan-loaded Mφs were then washed with Laurdan-free medium and imaged to establish the average GP value of the cells in the absence of Hc. Time-lapse sequences of images were acquired throughout Hc contact, interaction and internalization by Mφs. Time-lapse image sequences of Laurdan-labeled Mφs were acquired in a Zeiss LSM 510 META NLO microscope (Zeiss, Germany). Images were acquired simultaneously in four channels. Channels 1 and 2 were used to acquire the Laurdan emitted fluorescence in 440 nm and 490 nm respectively, channel 3 was used to acquire transmitted light images of the Mφs as a reference and channel 4 was used to image the red fluorescence from Hc-labeled cells. To compare the lipid lateral organization at the Hc-macrophage contact areas to the average macrophage lipid organization, we calculated the entire GP sequence from the time-lapse experiment and the average GP values for the Mφs is calculated for each frame. To follow lipid organization changes specifically at the site of Hc interaction, masks were obtained for each frame, representing the position of each Hc cell along the interaction process using the fluorescence images in channel 4. The masks were applied over the GP sequence and the average GP values for Hc contact sites were obtained for each frame. All images were acquired with a Zeiss Plan-Apochromat 63x/1.40 oil immersion objective lens.

Laurdan was excited by two-photon excitation, using a MaiTai Titanium-Saphire pulsed laser (80 MHz pulse frequency, 120 fs pulse width) (Spectra-Physics Newport, Mountain View, California) at 780 nm using a 680LP dichroic mirror and fluorescence emission was measured at 440 nm and 490 nm, simultaneously at the META spectral detector. The emission wavelengths at the META detector were set carefully to avoid cross talk from other fluorescence signals from the cells. Hc-Rho yeasts were used for these experiments and fluorescence was excited at 561 nm and emission was observed through a BP 575-615 IR band pass filter and collected in the photomultiplier tube at channel four. Transmitted light images of the cells were acquired during all the measurements using the 561 nm laser line simultaneously to the acquisition of the Hc-Rho image. After time-lapse sequences acquisition, GP images were calculated for each frame from the images obtained at 440 nm and 490 nm, as described before (Parasassi *et al.*, 1991), using equation 1 as follows:

$$GP_{corr} = \frac{(I_{440} - G \times I_{490})}{(I_{440} + G \times I_{490})} \quad (1)$$

I_{440} is the pixel intensity at 440 nm and I_{490} corresponds to the pixel intensity at 490 nm. The G factor is used to correct possible differences in sensitivity between the two channels and is obtained from images collected in the same experimental conditions for a Laurdan solution (20 mM) in DMSO, where the GP is known to be 0.2 (Sanchez *et al.*, 2007). Images were analyzed and GP calculations were performed in SimFCS software (Laboratory for Fluorescence Dynamics, University of California at Irvine, California, USA).

Laurdan GP images presented are from a representative experiment of three replicates. As described above, Mφs values are calculated as the average of all Laurdan signals in the image, meaning that all macrophages are being included. In our experiments all Mφs cells in all images are in contact with at least one Hc cell. All Hc cells detected in the field are measured as a contact area, as described above. Then, considering approximately 30 Hc cells and at least 20 Mph cells detected per field, in 90 frames, we have about 2700 measurements of Hc-Mφs contact regions per experiment, more than 60 Mph cells measured in the 3 replicates and about 90 contact regions followed in real time during the interaction process. It is worthy to note that the area of Mφs is much larger than the area of contact regions recovered from Hc-Rho fluorescence. As the area of the contact regions is much smaller, less pixels are used to calculate the average GP of this areas, and that is the reason of the larger variation observed for these values. Results were compared by unpaired t-test and considered significantly different for $p<0.001$. Statistics are presented in Supplementary Table 2.

Sterol enrichment at Mφs and Hc association sites.

To determine whether cholesterol is recruited to fungal binding sites J774.16 cells were used. Mφs were plated in 8-chamber polystyrene tissue-culture glass slides as described

previously (Nosanchuk *et al.*, 2003). Hc was incubated with wheat germ agglutinin (WGA)-Alexa 546 at 1 ug/mL at RT for 1h, washed three times with PBS and enumerated. Yeasts were added to the wells in a Hc:Mφ ratio of 5:1 and incubated for 15 min at 37 °C. After washing to remove non-adherent cells, the slides were stained with 10 ug/ml of filipin for 45 min at 4 °C. WGA and filipin are probes to detect chitin oligomers and sterol, respectively. The monolayers were washed again with PBS and fixed with PF 4% for 30 min at room temperature. Slides were mounted with *n*-propylgallate, sealed under a coverslip and then visualized by epifluorescence under an Observer Z1 microscope (Zeiss). After Z-stack acquisition, images were treated by deconvolution (Zen software - Zeiss).

Methyl-β-cyclodextrin (m-β-CD) treatment and association index.

To deplete sterol from cell surfaces, J774.16 Mφ monolayers were treated with m-*β*-CD. The m-*β*-CD stocks were prepared in serum-free DMEM. Mφs were washed once with serum-free DMEM and then incubated with different concentrations of m-*β*-CD (5, 10 or 20 mM) for 45 min at 37 °C. After washing with serum-free medium, Mφs were used for functional assays. Different concentrations of m-*β*-CD were used based on previous studies showing that increasing concentrations reduce sterol content in a dose-dependent fashion (Ottico *et al.*, 2003). After m-*β*-CD treatment, sterol depletion was confirmed by staining Mφs with filipin, a fluorescent sterol ligand. Cells were visualized by epifluorescence on a Zeiss Axioskop 200 inverted microscope equipped with a cooled CCD using 63x and 40x objectives. Cell viability after m-*β*-CD treatment was assessed as described (Abboud *et al.*, 2009).

To measure the impact of cholesterol depletion on association, Mφs plated onto 24-well plates were cultivated with or without m-*β*-CD under the conditions detailed above. After m-*β*-CD treatment Mφs were washed with PBS 3 times and then incubated with GFP-Hc for 15 or 45 min at 37 °C (multiplicity of infection 5 Hc: 1 Mφ). Plates were washed and infected Mφs displaying fluorescent yeast were measured using a FACSCalibur flow cytometer (BD Biosciences). Expression of CD18 was compared between control and m-*β*-CD treated cells also using flow cytometry. For these experiments, Mφs (lxlO^6 cells) were detached from flasks using 0.053 mM EDTA at room temperature for 5 minutes and then washed again with PBS. Cells were fixed with PF 4% for 30 min at room temperature. After blocking non-specific sites using 1% BSA, anti-mouse PE-conjugated CD18 (1μg/mL) (Biolegend, clone M18/2) or anti-mouse APC-conjugated CD11b (1μg/mL) (eBioscience, clone M1/70) was added and the cells incubated for 1 hour at room temperature. Negative isotype controls (IgG1 and IgG2a antibodies conjugated to APC, BIO-RAD) were used as controls. A total of 10,000 events were recorded for each flow cytometer analysis. The percentage of Hc-associated Mφs and the association index (total number of Mφs containing Hc adhered and/or internalized) was obtained for each experimental condition (Cordero *et al.*, 2016). All experiments were performed three times with consistent results. A control experiment without m-*β*-CD treatment was performed and the infection rate normalized as 100%.

Optical Tweezers experiments.

We used optical tweezers to access the interaction between Hc and Mφs. All the experimental procedures used were adapted from (Guimaraes *et al.*, 2011). Briefly, a yeast

cell suspension was trapped with the optical tweezers and allowed to interact with an adhered Mφ for periods of time ranging from 5 to 300 s. Then, the microscope stage was set to move with a controlled velocity in order to detach the optically trapped yeast cell from the Mφ surface. The maximum optical force in these experiments was set to be in the order of 20 pN (Viana *et al.*, 2007). If the Hc-host cell interactions were stronger than the maximum force the cells remain in contact and we considered this event as a positive adhesion event. The relative adhesion was defined as the number of positive adhesion events (N) divided by the total number of attempts (N_0). The relative adhesion was determined for each time point and each experimental condition used. The characteristic time (τ) was defined as the time required for 63% of the interactions to be positive in all the attempts tested and it was determined based on the best fit for all the curves obtained according to the equation:

$$\frac{N}{N_0} = 1 - exp\left(-\frac{t}{\tau}\right) \quad (2)$$

The error bars in the relative adhesion were determined as half the difference between the maximum and minimum values for each time interval in 30 events performed with 3 different samples. The error bars in the characteristic time were obtained using the best curve fit for Equation (2) and also weighting the data with the errors for the relative adhesion. All curve fits were obtained using the Kaleidagraph software (Synergy Software). To investigate the sterol requirement four experimental conditions were used: (i) Hc with control Mφs. (ii) Hc with 10 mM m-β-CD treated Mφs, (iii) opsonized Hc with control Mφs, and (iv) opsonized Hc with 10 mM m-β-CD treated Mφs. To determine the influence of GSL Mφs were treated with P4 as described below. Requirement of CD18 was studied using Mφs expressing very low amounts of this integrin (Sorgi *et al.*, 2009) and for the co-receptors of distinct integrins, we have used CHO cells transfected with LFA-1 (CD18/CD11a), CR1 (CD35), CR3 (CD18/CD11b) or CR4 (CD18/CD11c).

Influence of m-β-CD and CtxB on phagocytosis of Hc by Mφs.

We tested whether m-β-CD influenced internalization of Hc by Mφs according to our previously published protocol, with minor adaptations (Shi *et al.*, 2008). Briefly, Mφs were plated at 2×10^5 cells/well in an eight-chamber polystyrene tissue-culture glass slide (Becton Dickinson) and grown overnight. Hc were pre-incubated with 8 μg/ml NHS-Rho (Molecular Probes) at 4 °C for 1 h. After several washes with PBS to remove excess NHS-Rho, fungal cells were plated onto Mφ monolayers, with or without m-β-CD treatment, as described previously. Cells were then moved back to 37 °C and incubated with NHS-Rho-labeled Hc (Hc-Rho). After incubation, non-attached Hc were removed by washing the preparation with PBS. The monolayers were then incubated with Uvitex B (100μg/ml in PBS), a fluorescent dye that binds specifically to chitin on the Hc cell wall. Cells were washed again with PBS and then fixed with PF 4% for 30 min at room temperature. To evaluate the effect of fungal opsonization during this interaction, Hc were incubated with MAb to HSP60 (50 μg/mF of

mAh) and then added to the Mφ monolayer. After fixing with PF 4%, the slides were washed with PBS, sealed under a coverslip and visualized by epifluorescence. All yeast cells fluoresced red and only non-internalized Hc also fluoresced blue, since Uvitex B is excluded from live Mφs (Levitz *et al.*, 1987). In each system at least 300 Mφs were counted and the percentage of association number was determined. From infected Mφs, we determined the percentage of adherent and internalized Hc.

P4 treatment of Mφs.

To estimate the participation of GSL expressed at Mφ surface during interaction with Hc, we inhibited GlcCer formation, the first step during gangliosides biosynthesis (Fox *et al.*, 2001). Mφs were incubated for three days with 1 μM P4r, a small molecular weight inhibitor of the enzyme ceramide:glucosyltransferase (Cer:GlcT). After treatment, Mφs were washed with serum-free medium and used to interact with GFP-Hc as described. The association index (total number of Mφs containing Hc adhered and/or internalized) was obtained for each experimental condition as described above. Control experiments used an inactive isomer, P4s. OT experiments were developed as mentioned above. The expression of gangliosides after P4r treatment was determined (see below) and compared with control. P4r and P4s were synthesized by Dr. D. Meyers, Synthetic Core Facility, The Johns Hopkins School of Medicine. To evaluate the effect of P4 on the cytoskeleton, Mφs were plated at 5×10^5 cells/well in an eight-chamber polystyrene tissue-culture glass slide (Becton Dickinson) and treated with P4r or P4s as described above. After three days of treatment cells were washed with PBS and then incubated with phalloidin-FITC (Sigma-Aldrich) and DAPI (1 μg/ml) (Sigma-Aldrich) for 1 hour. Mφs were washed with PBS, slides were mounted with *n*-propylgallate, sealed under a coverslip and then visualized by epifluorescence under an Observer Z1 microscope (Zeiss). Experiments were performed twice with consistent results.

Lipid extraction.

Total lipids were extracted according to Schnaar (Schnaar *et al.*, 1994). Mφs with or without P4r (1-phenyl-2-palmitoylamino-3-pyrrolidino-1-propanol) or m-*β*-CD were washed with cold PBS and removed from the Petri dishes with a scrapper. The cells were collected by centrifugation at 4 °C and suspended in 3 ml of ice-cold water (W). Eight ml of methanol (M) was added and the suspension vigorously mixed. Chloroform (C) (4 ml) was added to the system reaching a final proportion of C-M-W (4:8:3). After two hours under agitation at room temperature the suspension was centrifuged and the pellet extracted again with the same solvent mixture (C-M-W; 4:8:3). The pellet was dried at room temperature and then solubilized with 3-5 mL of NaOH 0.1 M and the total protein content was determined using Pierce BCA Protein Assay Kit (Thermo Fischer Scientific, US). Protein content was used to normalize the samples. The lipidic extracts were combined and water was added to the supernatant to reach a final concentration of C-M-W (4:8:5.6). The suspension was mixed and a biphasic system formed. The upper phase containing the polar lipids, including the gangliosides, was submitted to reverse phase chromatography (tC18 SepPak Plus cartridges) to remove salts and other polar contaminants. Cartridges were previously washed with 3 ml of water, M-W (1:1), methanol and M-W (1:1) again. The upper phase was loaded and the cartridges washed with 3 ml of M-W (1:2) and M-W (1:1). GSL were eluted with 3 ml of methanol. The methanol eluant (from the upper phase) and the whole lower phase, enriched

in ceramide and sphingomyelin, were dried under N2 and resolved by thin layer chromatography as described below.

Thin layer chromatography (TLC).

The fraction eluted in methanol was solubilized in C-M-W (4:8:3) and the lower phase was solubilized in chloroform. Samples were then spotted onto TLC plates. TLC was performed on silica gel plates in proper solvent systems according to each class of lipids to be investigated. Ceramide analysis was developed in a solvent system consisting of C-M-W (80:10:1) (van Echten-Deckert, 2000). Cupric sulfate in aqueous phosphoric acid was sprayed over the TLC plate for further band visualization after heating at 180 °C for 15 min. Lipid bands, including ceramide, appear brown against a white background (van Echten-Deckert, 2000). Ceramide from bovine brain was used as a standard. To identify sphingomyelin the lipids from lower phase were resolved using C-M-W (65:25:4). TLCs were exposed to iodine in chambers saturated with iodine crystals. Bands appear yellow against a white background. Sphingomyelin from bovine brain was used as a standard. Gangliosides were resolved in solvent system containing C-M-0.25% aqueous KCl (60:35:8) (Schnaar *et al.*, 1994). Plates were sprayed with resorcinol/HCl reagent and heated at 125 °C for 20 min (Schnaar *et al.*, 1994). Gangliosides were visualized as purple spots. A mixture containing bovine brain gangliosides was used as a standard.

Immunostaining of gangliosides.

To confirm the presence of GM1 and GD1a (respectively mono and disialo- species of gangliosides) on lipid extracts of J774.16 Mφs, we performed an immunostaining assay using monoclonal antibodies to GM1 and GD1a (Schnaar *et al.*, 2002). GSL were resolved by TLC as above and the plate was dipped in a solution of 0.2% polyisobutyl methacrylate (Aldrich) in hexane for 30s. The plate was dried, sprayed with PBS and blocked for nonspecific binding with 10 mg/ml BSA in PBS for 1 h at room temperature. After washing with PBS three times, the plate was incubated with antibodies to the gangliosides (2 μg/ml) for 2 h at room temperature followed by incubation with a secondary alkaline phosphatase-conjugated anti-mouse IgG (1 μg/ml) under the same conditions. The plate was washed three times with PBS and then developed by using Sigma Fast NBT-BCIP according to the manufacturer's instructions. Reactive bands (purple) were compared with standards resolved at the same time and conditions, but developed with resorcinol/HCl reagent.

Influence of P4, complex gangliosides, CD11b, CD18, CtxB and oligo-GM1 during Mφs and Hc association.

GM1-oligosaccharides (oligo-GM1) were generated by treatment of GM1 with a specific ceramide glycanase (Calbiochem) (Zhou *et al.*, 1989). To investigate whether P4 treatment, absence of complex gangliosides, CD11b and CD18 are required for Mφs to associate with Hc, we used primary Mφs treated with P4 and Mφs derived from *B4galnt1*$^{-/-}$, CD11b$^{-/-}$ or CD18^{low} mice. CtxB is a standard ligand for GM1 and has been extensively used as a lipid raft marker (Vyas *et al.*, 2001). To access the effect of CTxB, we treated Mφs with 1 μg/ml of CTxB for 45 min at 4 °C before incubation with Hc. According to the manufacturer, this concentration achieves 50% saturation of GM1-coated plates. Mφs were washed with PBS 3 times and then incubated with GFP-Hc for 45 min at 37 °C (multiplicity of infection 5 Hc: 1

Mφ). In another set of experiments, oligo-GM1 and GFP-Hc were co-incubated with Mφs for 1h. Association indexes were determined by flow cytometry as described above (Cordero *et al.*, 2016). In addition, some systems where fungal cells were opsonized with anti-HSP60 (13B7 or 7B6 (Guimaraes *et al.*, 2009)) or M antigen specific mAbs (Guimaraes *et al.*, 2008) were also tested to evaluate whether opsonization would impact infection. The percentage of associated Mφs was obtained for each experimental condition. All experiments were performed three times with consistent results.

Lipid microdomains isolation and dot-blot experiments.

To analyze the content of CD18 and CD14 in lipid microdomains, we used bone marrow-derived Mφs from wild-type and *B4galnt1*$^{-/-}$ mice. The protocol published by Takeushi and colleagues was used to prepare the Mφs (Takeuchi *et al.*, 1999). Briefly, femur and tibia were removed, the tissue removed by scalping and briefly washed in 70% ethanol. After cutting both sides, the bone marrow was flushed with PBS and cells gently homogenized. Precursors cells were seeded at 2×10^6 per 100-mm dish in 10 ml complete medium (DMEM, supplemented with 10% FCS, 1-glutamine, HEPES, β_2-mercaptoethanol, and penicillin/streptomycin) with 20% conditioned medium (containing M-CSF) harvested from L929 fibroblast cultured cells. After seven days Mφs were harvested and used to prepare lipid microdomains according to DeBruin and colleagues (DeBruin *et al.*, 2005) with minor modifications. Cells were washed in TNE buffer (25 mM Tris/HCl (pH 7.4), 150 mM NaCl) and the pellets lysed in 250 μl of the same buffer containing 1% triton-X-100 and a protease inhibitor cocktail (Sigma) for 30 min at 4°C. Lysates were mixed with equal volume of 80% sucrose (w/v) in TNE buffer and then transferred to a SW41 centrifuge tube. The samples was homogenized an then overlaid sequentially with 40% (3.5 ml), 35% (5 ml) and 5% (3.5 ml) of sucrose in TNE and centrifuged at 100,000*g* for 18 h at 4°C. Eleven fractions of 1 ml each were sequentially collected from the top and analyzed for the presence of GM1 (lipid raft marker), CD14 and CD18. Aliquots of each fraction were spotted on nitrocellulose membrane (Millipore, Bedford, MA) by using a dot-blot equipment (Pharmacia, US). Fraction twelve, overloaded with non-rafts proteins, was not spotted. After blocking, the membrane was overlaid with peroxidase-linked CtxB or monoclonal antibodies to CD14 and CD18 (BD Biosciences), followed by a secondary conjugated to peroxidase. Membranes were washed, and developed by enhanced chemiluminescence (Pierce, Rockford, IL) or DAB peroxidase solution. The spots were quantified using the ImageJ software (NIH).

Surface distribution of GM1, CD18 and CD11b during interaction of Hc and Mφs.

To determine whether GM1 was recruited to fungal binding sites at the bone marrow-derived Mφ surface, labeling with FITC-conjugated CtxB was used. Mφs were plated in 8-chamber polystyrene tissue-culture glass slides as described previously (Nosanchuk *et al.*, 2003). Hc previously incubated with Uvitex 2B (Chaka *et al.*, 1995) were added to the wells in a Hc:Mφ ratio of 5:1 and incubated for 15 or 45 min at 37 °C. After washing to remove non-adherent cells, the slides were incubated with FITC-conjugated CtxB (1μg/ml in PBS-BSA 1%) for 45 min at 4 °C. The monolayers were washed again with PBS and fixed with PF 4% for 30 min at room temperature. After blocking non-specific sites using 1% BSA, anti-mouse CD18 (1μg/mL) (BD Bioscience) or and anti-mouse CD11b (1μg/mL) (BD Bioscience) were separately incubated in different slides for 1 hour at room temperature.

After extensive washing, a Goat anti-IgG Alexa 546 (Invitrogen) was incubated for 1 hour. Slides were mounted with *n*-propylgallacte, sealed under a coverslip and then visualized by epifluorescence under an Observer Z1 microscope (Zeiss). After Z-stack acquisition, images were treated by deconvolution (Zen software - Zeiss).

CD18 levels in macrophages from wild type and B4galnt1$^{-/-}$ mice

Mφs from wild-type and *B4galnt1*$^{-/-}$ mice (1×10^6 cells) were incubated with PE-conjugated anti-mouse CD18 as described above and 10,000 events were recorded for flow cytometer analysis. All experiments were performed three times with consistent results.

Statistical analysis.

All statistical analyses were performed using GraphPad Prism 6, version 5.02 for Windows (GraphPad Software).

Supplementary Material

Refer to Web version on PubMed Central for supplementary material.

ACKNOWLEDGEMENTS

A.J.G. and L.N. were supported in part by an Interhemispheric Research Training Grant in Infectious Diseases, Fogarty International Center (NIH D43-TW007129). A.J.G and J.D.N. were supported in part by NIH AI056070-01A2 and the Center for AIDS Research at the Albert Einstein College of Medicine and Montefiore Medical Center (NIH AI-51519). A.J.G., L.N., M.L.R., B.P., N.BV. and D.Z-M. are supported by grants from Conselho Nacional de Desenvolvimento Tecnologico (CNPq, Brazil) and Fundação Carlos Chagas Filho de Amparo à Pesquisa do Estado do Rio de Janeiro (FAPERJ, Brazil). LN was also supported by CAPES-Fulbright (Visiting Scientist/Visiting Professor Scholar Program). Mutant mice and ganglioside oligosaccharides were generated with support from the National Institutes of Health (NS037096). The authors thank Dr. Steven U. Walkley (Department of Neuroscience, AECOM) and Lucia Faccioli (USP, Riberião Preto) for kindly provide us with *B4galnt1*$^{-/-}$ and CD18^{low} mice, respectively. The authors state that there are no conflicts of interests.

References

Abboud N, De Jesus M, Nakouzi A, Cordero RJ, Pujato M, Fiser A, et al. (2009). Identification of linear epitopes in Bacillus anthracis protective antigen bound by neutralizing antibodies. J Biol Chem 284, 25077–25086. [PubMed: 19617628]

Allendoerfer R, Biovin GP and Deepe GS Jr. (1997). Modulation of immune responses in murine pulmonary histoplasmosis. J Infect Dis 175, 905–914. [PubMed: 9086148]

Ando S and Yu RK (1984). Fatty acid and long-chain base composition of gangliosides isolated from adult human brain. Journal of neuroscience research 12, 205–211. [PubMed: 6502750]

Barrias ES, Dutra JM, De Souza W and Carvalho TM (2007). Participation of macrophage membrane rafts in Trypanosoma cruzi invasion process. Biochem Biophys Res Commun 363, 828–834. [PubMed: 17904520]

Bergelson LD, Bukrinskaya AG, Prokazova NV, Shaposhnikova GI, Kocharov SL, Shevchenko VP, et al. (1982). Role of gangliosides in reception of influenza virus. Eur J Biochem 128, 467–474. [PubMed: 7151789]

Brown DA and London E (2000). Structure and function of sphingolipid- and cholesterol-rich membrane rafts. J Biol Chem 275, 17221–17224. [PubMed: 10770957]

Bullock WE and Wright SD (1987). Role of the adherence-promoting receptors, CR3, LFA-1, and p150,95, in binding of Histoplasma capsulatum by human macrophages. J Exp Med 165, 195–210. [PubMed: 3025331]

Cano MV and Hajjeh RA (2001). The epidemiology of histoplasmosis: a review. Semin Respir Infect 16, 109–118. [PubMed: 11521243]

Chaka W, Scharringa J, Verheul AF, Verhoef J, Van Strijp AG and Hoepelman IM (1995). Quantitative analysis of phagocytosis and killing of Cryptococcus neoformans by human peripheral blood mononuclear cells by flow cytometry. Clinical and diagnostic laboratory immunology 2, 753–759. [PubMed: 8574842]

Cordero RJ, Liedke SC, de SAGR, Martinez LR, Nimrichter L, Frases S, et al. (2016). Enhanced virulence of Histoplasma capsulatum through transfer and surface incorporation of glycans from Cryptococcus neoformans during co-infection. Scientific reports 6, 21765. [PubMed: 26908077]

Cuschieri J, Billigren J and Maier RV (2006). Endotoxin tolerance attenuates LPS-induced TLR4 mobilization to lipid rafts: a condition reversed by PKC activation. J Leukoc Biol 80, 1289–1297. [PubMed: 16959900]

Das T, Sa G, Hilston C, Kudo D, Rayman P, Biswas K, et al. (2008). GM1 and tumor necrosis factor-alpha, overexpressed in renal cell carcinoma, synergize to induce T-cell apoptosis. Cancer Res 68, 2014–2023. [PubMed: 18339884]

Day CA and Kenworthy AK (2015). Functions of cholera toxin B-subunit as a raft cross-linker. Essays in biochemistry 57, 135–145. [PubMed: 25658350]

DeBruin LS, Haines JD, Wellhauser LA, Radeva G, Schonmann V, Bienzle D and Harauz G (2005). Developmental partitioning of myelin basic protein into membrane microdomains. J Neurosci Res 80, 211–225. [PubMed: 15772981]

Dickens BF and Thompson GA Jr. (1981). Rapid membrane response during low-temperature acclimation. Correlation of early changes in the physical properties and lipid composition of Tetrahymena microsomal membranes. Biochim Biophys Acta 644, 211–218. [PubMed: 6789874]

Dykstra M, Cherukuri A, Sohn HW, Tzeng SJ and Pierce SK (2003). Location is everything: lipid rafts and immune cell signaling. Annu Rev Immunol 21, 457–481. [PubMed: 12615889]

Ehlers MR (2000). CR3: a general purpose adhesion-recognition receptor essential for innate immunity. Microbes and infection / Institut Pasteur 2, 289–294.

Fortier AH and Falk LA (2001). Isolation of murine macrophages. Curr Protoc Immunol Chapter 14, Unit 14 11.

Fox DA, He X, Abe A, Hollander T, Li LL, Kan L, et al. (2001). The T lymphocyte structure CD60 contains a sialylated carbohydrate epitope that is expressed on both gangliosides and glycoproteins. Immunol Invest 30, 67–85. [PubMed: 11465673]

Gatfield J and Pieters J (2000). Essential role for cholesterol in entry of mycobacteria into macrophages. Science 288, 1647–1650. [PubMed: 10834844]

Gaus K, Gratton E, Kable EP, Jones AS, Gelissen I, Kritharides L and Jessup W (2003). Visualizing lipid structure and raft domains in living cells with two-photon microscopy. Proceedings of the National Academy of Sciences of the United States of America 100, 15554–15559. [PubMed: 14673117]

Goluszko P, Popov V, Wen J, Jones A and Yallampalli C (2008). Group B streptococcus exploits lipid rafts and phosphoinositide 3-kinase/Akt signaling pathway to invade human endometrial cells. Am J Obstet Gynecol 199, 548 e541–549. [PubMed: 18486087]

Grassme H, Jendrossek V, Riehle A, von Kurthy G, Berger J, Schwarz H, et al. (2003). Host defense against Pseudomonas aeruginosa requires ceramide-rich membrane rafts. Nat Med 9, 322–330. [PubMed: 12563314]

Guimaraes AJ, Frases S, Gomez FJ, Zancope-Oliveira RM and Nosanchuk JD (2009). Monoclonal antibodies to heat shock protein 60 alter the pathogenesis of Histoplasma capsulatum. Infection and immunity 77, 1357–1367. [PubMed: 19179416]

Guimaraes AJ, Frases S, Pontes B, de Cerqueira MD, Rodrigues ML, Viana NB, et al. (2011). Agglutination of Histoplasma capsulatum by IgG monoclonal antibodies against Hsp60 impacts macrophage effector functions. Infection and immunity 79, 918–927. [PubMed: 21134968]

Guimaraes AJ, Hamilton AJ, de MGHL, Nosanchuk JD and Zancope-Oliveira RM (2008). Biological function and molecular mapping of M antigen in yeast phase of Histoplasma capsulatum. PloS one 3, e3449. [PubMed: 18927619]

Hakomori S (2003). Structure, organization, and function of glycosphingolipids in membrane. Curr Opin Hematol 10, 16–24. [PubMed: 12483107]

Huang JH, Lin CY, Wu SY, Chen WY, Chu CL, Brown GD, et al. (2015). CR3 and Dectin-1 Collaborate in Macrophage Cytokine Response through Association on Lipid Rafts and Activation of Syk-JNK-AP-1 Pathway. PLoS pathogens 11, e1004985. [PubMed: 26132276]

Huang SH, Wu CH, Chang YC, Kwon-Chung KJ, Brown RJ and Jong A (2012). Cryptococcus neoformans-derived microvesicles enhance the pathogenesis of fungal brain infection. PloS one 7, e48570. [PubMed: 23144903]

Ilangumaran S and Hoessli DC (1998). Effects of cholesterol depletion by cyclodextrin on the sphingolipid microdomains of the plasma membrane. Biochem J 335 (Pt 2), 433–440. [PubMed: 9761744]

Jia F, Howlader MA and Cairo CW (2016). Integrin-mediated cell migration is blocked by inhibitors of human neuraminidase. Biochimica et biophysica acta 1861, 1170–1179. [PubMed: 27344026]

Jimenez-Lucho V, Ginsburg V and Krivan HC (1990). Cryptococcus neoformans, Candida albicans, and other fungi bind specifically to the glycosphingolipid lactosylceramide (Gal beta 1-4Glc beta 1-1Cer), a possible adhesion receptor for yeasts. Infect Immun 58, 2085–2090. [PubMed: 2194958]

Kainu V, Hermansson M and Somerharju P (2010). Introduction of phospholipids to cultured cells with cyclodextrin. Journal of lipid research 51, 3533–3541. [PubMed: 20881052]

Kalischuk LD, Inglis GD and Buret AG (2009). Campylobacter jejuni induces transcellular translocation of commensal bacteria via lipid rafts. Gut Pathog 1, 2. [PubMed: 19338680]

Kansau I, Berger C, Hospital M, Amsellem R, Nicolas V, Servin AL and Bernet-Camard MF (2004). Zipper-like internalization of Dr-positive Escherichia coli by epithelial cells is preceded by an adhesin-induced mobilization of raft-associated molecules in the initial step of adhesion. Infect Immun 72, 3733–3742. [PubMed: 15213113]

Kasai R, Kitajima Y, Martin CE, Nozawa Y, Skriver L and Thompson GA Jr. (1976). Molecular control of membrane properties during temperature acclimation. Membrane fluidity regulation of fatty acid desaturase action? Biochemistry 15, 5228–5233. [PubMed: 826267]

Kauffman CA (2009). Histoplasmosis. Clin Chest Med 30, 217–225, v. [PubMed: 19375629]

Kim S, Watarai M, Makino S and Shirahata T (2002). Membrane sorting during swimming internalization of Brucella is required for phagosome trafficking decisions. Microb Pathog 33, 225–237. [PubMed: 12473437]

Krivan HC, Ginsburg V and Roberts DD (1988a). Pseudomonas aeruginosa and Pseudomonas cepacia isolated from cystic fibrosis patients bind specifically to gangliotetraosylceramide (asialo GM1) and gangliotriaosylceramide (asialo GM2). Arch Biochem Biophys 260, 493–496. [PubMed: 3124753]

Krivan HC, Roberts DD and Ginsburg V (1988b). Many pulmonary pathogenic bacteria bind specifically to the carbohydrate sequence GalNAc beta 1-4Gal found in some glycolipids. Proc Natl Acad Sci U S A 85, 6157–6161. [PubMed: 3413084]

Kroken AR, Karalewitz AP, Fu Z, Baldwin MR, Kim JJ and Barbieri JT (2011). Unique ganglioside binding by botulinum neurotoxins C and D-SA. The FEBS journal 278, 4486–4496. [PubMed: 21554541]

Lafont F and van der Goot FG (2005). Bacterial invasion via lipid rafts. Cell Microbiol 7, 613–620. [PubMed: 15839890]

Levitz SM, DiBenedetto DJ and Diamond RD (1987). A rapid fluorescent assay to distinguish attached from phagocytized yeast particles. Journal of immunological methods 101, 37–42. [PubMed: 3112238]

Lin JS, Huang JH, Hung LY, Wu SY and Wu-Hsieh BA Distinct roles of complement receptor 3, Dectin-1, and sialic acids in murine macrophage interaction with Histoplasma yeast. J Leukoc Biol 88, 95–106. [PubMed: 20360401]

Lin JS, Huang JH, Hung LY, Wu SY and Wu-Hsieh BA (2010). Distinct roles of complement receptor 3, Dectin-1, and sialic acids in murine macrophage interaction with Histoplasma yeast. Journal of leukocyte biology 88, 95–106. [PubMed: 20360401]

Long KH, Gomez FJ, Morris RE and Newman SL (2003). Identification of heat shock protein 60 as the ligand on Histoplasma capsulatum that mediates binding to CD18 receptors on human macrophages. Journal of immunology 170, 487–494.

Lopez PH and Schnaar RL (2006). Determination of glycolipid-protein interaction specificity. Methods Enzymol 417, 205–220. [PubMed: 17132507]

Marsh D (2009). Cholesterol-induced fluid membrane domains: a compendium of lipid-raft ternary phase diagrams. Biochim Biophys Acta 1788, 2114–2123. [PubMed: 19699712]

Martin CE, Hiramitsu K, Kitajima Y, Nozawa Y, Skriver L and Thompson GA (1976). Molecular control of membrane properties during temperature acclimation. Fatty acid desaturase regulation of membrane fluidity in acclimating Tetrahymena cells. Biochemistry 15, 5218–5227. [PubMed: 826266]

Matrosovich M, Herrler G and Klenk HD (2015). Sialic Acid Receptors of Viruses. Topics in current chemistry 367, 1–28. [PubMed: 23873408]

Maza PK, Straus AH, Toledo MS, Takahashi HK and Suzuki E (2008). Interaction of epithelial cell membrane rafts with Paracoccidioides brasiliensis leads to fungal adhesion and Src-family kinase activation. Microbes Infect 10, 540–547. [PubMed: 18403242]

Murphy SC, Hiller NL, Harrison T, Lomasney JW, Mohandas N and Haldar K (2006). Lipid rafts and malaria parasite infection of erythrocytes. Mol Membr Biol 23, 81–88. [PubMed: 16611583]

Nakayama H, Yoshizaki F, Prinetti A, Sonnino S, Mauri L, Takamori K, et al. (2008). Lyn-coupled LacCer-enriched lipid rafts are required for CD11b/CD18-mediated neutrophil phagocytosis of nonopsonized microorganisms. J Leukoc Biol 83, 728–741. [PubMed: 18055569]

Newman SL (1999). Macrophages in host defense against Histoplasma capsulatum. Trends Microbiol 7, 67–71. [PubMed: 10081083]

Newman SL, Bucher C, Rhodes J and Bullock WE (1990). Phagocytosis of Histoplasma capsulatum yeasts and microconidia by human cultured macrophages and alveolar macrophages. Cellular cytoskeleton requirement for attachment and ingestion. The Journal of clinical investigation 85, 223–230. [PubMed: 2104879]

Nicholson KM, Quinn DM, Kellett GL and Warr JR (1999). Preferential killing of multidrug-resistant KB cells by inhibitors of glucosylceramide synthase. Br J Cancer 81, 423–430. [PubMed: 10507766]

Nosanchuk JD, Steenbergen JN, Shi L, Deepe GS Jr. and Casadevall A (2003). Antibodies to a cell surface histone-like protein protect against Histoplasma capsulatum. The Journal of clinical investigation 112, 1164–1175. [PubMed: 14561701]

O'Brien XM, Heflin KE, Lavigne LM, Yu K, Kim M, Salomon AR and Reichner JS (2012). Lectin site ligation of CR3 induces conformational changes and signaling. The Journal of biological chemistry 287, 3337–3348. [PubMed: 22158618]

Oda M, Terao Y, Sakurai J and Nagahama M (2015). Membrane-Binding Mechanism of Clostridium perfringens Alpha-Toxin. Toxins 7, 5268–5275. [PubMed: 26633512]

Ottico E, Prinetti A, Prioni S, Giannotta C, Basso L, Chigorno V and Sonnino S (2003). Dynamics of membrane lipid domains in neuronal cells differentiated in culture. J Lipid Res 44, 2142–2151. [PubMed: 12897192]

Paller AS, Arnsmeier SL, Chen JD and Woodley DT (1995). Ganglioside GT1b inhibits keratinocyte adhesion and migration on a fibronectin matrix. The Journal of investigative dermatology 105, 237–242. [PubMed: 7636307]

Pan B, Fromholt SE, Hess EJ, Crawford TO, Griffin JW, Sheikh KA and Schnaar RL (2005). Myelin-associated glycoprotein and complementary axonal ligands, gangliosides, mediate axon stability in the CNS and PNS: neuropathology and behavioral deficits in single- and double-null mice. Exp Neurol 195, 208–217. [PubMed: 15953602]

Pang H, Le PU and Nabi IR (2004). Ganglioside GM1 levels are a determinant of the extent of caveolae/raft-dependent endocytosis of cholera toxin to the Golgi apparatus. J Cell Sci 117, 1421–1430. [PubMed: 14996913]

Parasassi T, De Stasio G, d'Ubaldo A and Gratton E (1990). Phase fluctuation in phospholipid membranes revealed by Laurdan fluorescence. Biophysical journal 57, 1179–1186. [PubMed: 2393703]

Parasassi T, De Stasio G, Ravagnan G, Rusch RM and Gratton E (1991). Quantitation of lipid phases in phospholipid vesicles by the generalized polarization of Laurdan fluorescence. Biophysical journal 60, 179–189. [PubMed: 1883937]

Pfaller MA and Diekema DJ (2010). Epidemiology of invasive mycoses in North America. Critical reviews in microbiology 36, 1–53. [PubMed: 20088682]

Piel G, Piette M, Barillaro V, Castagne D, Evrard B and Delattre L (2007). Study of the relationship between lipid binding properties of cyclodextrins and their effect on the integrity of liposomes. Int J Pharm 338, 35–42. [PubMed: 17289314]

Riethmuller J, Riehle A, Grassme H and Gulbins E (2006). Membrane rafts in host-pathogen interactions. Biochimica et biophysica acta 1758, 2139–2147. [PubMed: 17094939]

Rodrigues ML, Nakayasu ES, Oliveira DL, Nimrichter L, Nosanchuk JD, Almeida IC and Casadevall A (2008). Extracellular vesicles produced by Cryptococcus neoformans contain protein components associated with virulence. Eukaryotic cell 7, 58–67. [PubMed: 18039940]

Sanchez SA, Tricerri MA, Gunther G and Gratton E (2007) Laurdan Generalized Polarization: from cuvette to microscope, Formatex, pp. 8.

Sanchez SAT, M.A.; Gunther G; Gratton E (2007) Laurdan Generalized Polarization: from cuvette to microscope, Formatex, pp. 8.

Schmitz G and Orso E (2002). CD14 signalling in lipid rafts: new ligands and co-receptors. Curr Opin Lipidol 13, 513–521. [PubMed: 12352015]

Schnaar RL, Fromholt SE, Gong Y, Vyas AA, Laroy W, Wayman DM, et al. (2002). Immunoglobulin G-class mouse monoclonal antibodies to major brain gangliosides. Anal Biochem 302, 276–284. [PubMed: 11878808]

Schnaar RL and Needham LK (1994). Thin-layer chromatography of glycosphingolipids. Methods in enzymology 230, 371–389. [PubMed: 7511203]

Sheikh KA, Sun J, Liu Y, Kawai H, Crawford TO, Proia RL, et al. (1999). Mice lacking complex gangliosides develop Wallerian degeneration and myelination defects. Proceedings of the National Academy of Sciences of the United States of America 96, 7532–7537. [PubMed: 10377449]

Shi L, Albuquerque PC, Lazar-Molnar E, Wang X, Santambrogio L, Gacser A and Nosanchuk JD (2008). A monoclonal antibody to Histoplasma capsulatum alters the intracellular fate of the fungus in murine macrophages. Eukaryotic cell 7, 1109–1117. [PubMed: 18487350]

Silvius JR (2003). Role of cholesterol in lipid raft formation: lessons from lipid model systems. Biochim Biophys Acta 1610, 174–183. [PubMed: 12648772]

Sorgi CA, Secatto A, Fontanari C, Turato WM, Belanger C, de Medeiros AI, et al. (2009). Histoplasma capsulatum cell wall {beta}-glucan induces lipid body formation through CD18, TLR2, and dectin-1 receptors: correlation with leukotriene B4 generation and role in HIV-1 infection. Journal of immunology 182, 4025–4035.

Strasser JE, Newman SL, Ciraolo GM, Morris RE, Howell ML and Dean GE (1999). Regulation of the macrophage vacuolar ATPase and phagosome-lysosome fusion by Histoplasma capsulatum. Journal of immunology 162, 6148–6154.

Sun J, Shaper NL, Itonori S, Heffer-Lauc M, Sheikh KA and Schnaar RL (2004). Myelin-associated glycoprotein (Siglec-4) expression is progressively and selectively decreased in the brains of mice lacking complex gangliosides. Glycobiology 14, 851–857. [PubMed: 15175257]

Superti F and Donelli G (1991). Gangliosides as binding sites in SA-11 rotavirus infection of LLC-MK2 cells. J Gen Virol 72 (Pt 10), 2467–2474. [PubMed: 1655958]

Takeuchi O, Hoshino K, Kawai T, Sanjo H, Takada H, Ogawa T, et al. (1999). Differential roles of TLR2 and TLR4 in recognition of gram-negative and gram-positive bacterial cell wall components. Immunity 11, 443–451. [PubMed: 10549626]

Thornton BP, Vetvicka V, Pitman M, Goldman RC and Ross GD (1996). Analysis of the sugar specificity and molecular location of the beta-glucan-binding lectin site of complement receptor type 3 (CD11b/CD18). Journal of immunology 156, 1235–1246.

Triantafilou M, Miyake K, Golenbock DT and Triantafilou K (2002). Mediators of innate immune recognition of bacteria concentrate in lipid rafts and facilitate lipopolysaccharide-induced cell activation. J Cell Sci 115, 2603–2611. [PubMed: 12045230]

Triantafilou M and Triantafilou K (2003). Receptor cluster formation during activation by bacterial products. J Endotoxin Res 9, 331–335. [PubMed: 14577851]

van Echten-Deckert G (2000). Sphingolipid extraction and analysis by thin-layer chromatography. Methods Enzymol 312, 64–79. [PubMed: 11070863]

Viana NB, Rocha MS, Mesquita ON, Mazolli A, Maia Neto PA and Nussenzveig HM (2007). Towards absolute calibration of optical tweezers. Phys Rev E Stat Nonlin Soft Matter Phys 75, 021914. [PubMed: 17358374]

Vieira KP, de Almeida e Silva Lima Zollner AR, Malaguti C, Vilella CA and de Lima Zollner R (2008). Ganglioside GM1 effects on the expression of nerve growth factor (NGF), Trk-A receptor, proinflammatory cytokines and on autoimmune diabetes onset in non-obese diabetic (NOD) mice. Cytokine 42, 92–104. [PubMed: 18329889]

Vieth JA, Kim MK, Pan XQ, Schreiber AD and Worth RG (2010). Differential requirement of lipid rafts for FcgammaRIIA mediated effector activities. Cellular immunology 265, 111–119. [PubMed: 20728077]

Vyas KA, Patel HV, Vyas AA and Schnaar RL (2001). Segregation of gangliosides GM1 and GD3 on cell membranes, isolated membrane rafts, and defined supported lipid monolayers. Biol Chem 382, 241–250. [PubMed: 11308022]

Watarai M, Makino S, Fujii Y, Okamoto K and Shirahata T (2002). Modulation of Brucella-induced macropinocytosis by lipid rafts mediates intracellular replication. Cell Microbiol 4, 341–355. [PubMed: 12067319]

Weber G and Farris FJ (1979). Synthesis and spectral properties of a hydrophobic fluorescent probe: 6-propionyl-2-(dimethylamino)naphthalene. Biochemistry 18, 3075–3078. [PubMed: 465454]

Williamson JR, Shanahan MO and Hochmuth RM (1975). The influence of temperature on red cell deformability. Blood 46, 611–624. [PubMed: 1174695]

Ywazaki CY, Maza PK, Suzuki E, Takahashi HK and Straus AH (2011). Role of host glycosphingolipids on Paracoccidioides brasiliensis adhesion. Mycopathologia 171, 325–332. [PubMed: 21057877]

Zhou B, Li SC, Laine RA, Huang RT and Li YT (1989). Isolation and characterization of ceramide glycanase from the leech, Macrobdella decora. J Biol Chem 264, 12272–12277. [PubMed: 2745442]

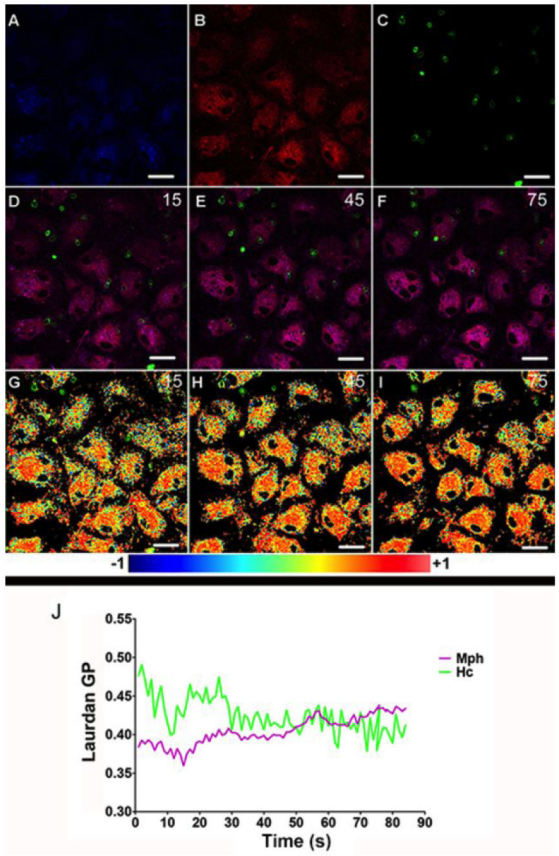

Figure 1 –. Hc yeast cells induce dynamic changes of lateral organization in Mφ membranes.

Hc-Rho yeast cells were plated onto bone marrow-derived murine Mφs previously stained with Laurdan. Images A (channel 1: 440 nm, arbitrarily colored blue), B (channel 2: 490 nm, arbitrarily colored red) and C (channel 3: 595 nm, arbitrarily colored green) depict the first frame displaying the interaction of Hc yeasts and Mφ. Merge images of the three channels are shown in three distinct time frames (15, 45 and 90 s of interaction; D-F). GP images at the same time frames merged with Hc-Rho images showing the increase in lateral organization over the time of interaction (G-I). GP values over this time course are depicted in panel J where the purple line represents average GP values of Mφ membranes and the green line represents the average GP specifically at the Hc-Mφ contact regions. Statistics were performed for (i) all frames, (ii) the first and last 10 minutes and for the (iii) three set of frames (30, 60 and 90). Representative of three independent experiments, differences considered significant by unpaired t-test. For all analyses $p<0.001$ (see details in Supplementary Table 2). Bar, 10 μm.

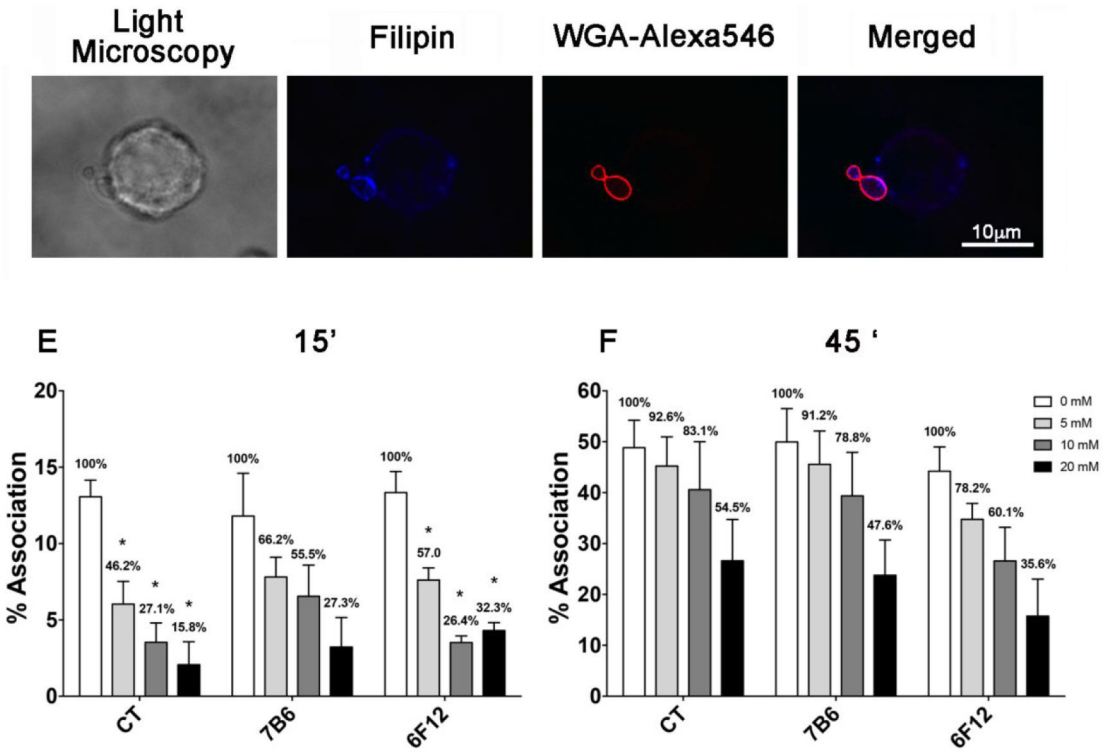

Figure 2 –. Importance of sterols in the Hc association with macrophages and effect of m-β-CD treatment on the association with Hc.

(A) Light microscopy of Mφ-Hc interaction. (B and C) Filipin staining of cholesterol in J774.16 Mφ membranes and WGA-Alexa546 in Hc. (D) Merged images denoting the co-localization of filipin staining and WGA-Alexa546-Hc. Bar, 10 μm. (E) GFP-Hc yeast cells with or without opsonization with antibodies to HSP60 (mAb 7B6) or to M antigen (mAb 6F12) were incubated for 15 or (F) 45 minutes with J774.16 Mφs pre-treated with different concentrations of m-β-CD. Samples were analyzed by flow cytometry. Bars show the percentage of yeast-associated Mφs over the total number of Mφs analyzed. The numbers on the bars indicate the total infected Mφs in each system followed by the percentage determined in the setting of infection compared to controls (considered as 100%). The results shown are the average of three independent experiments. Each individual system showed statistical significance ($P<0.0001$) in comparison to its appropriate control.

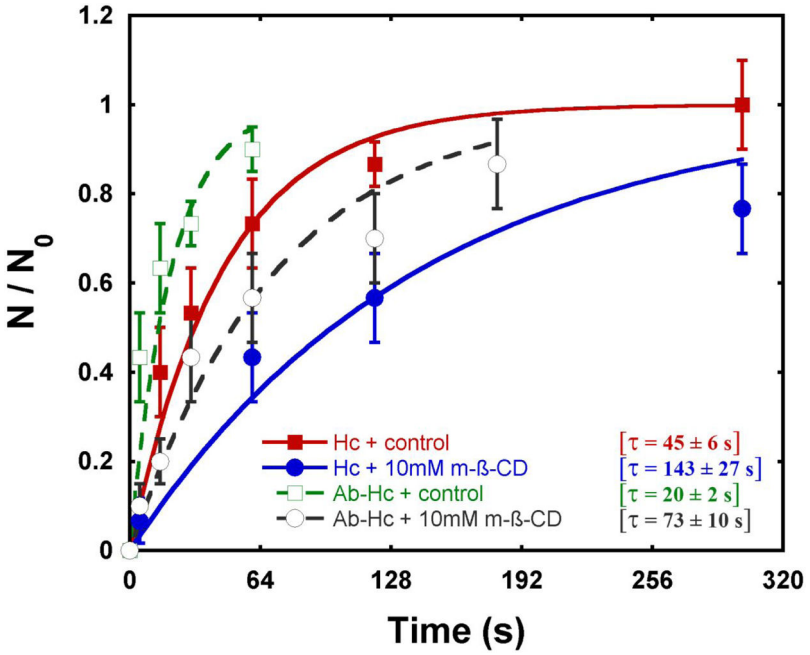

Figure 3 –. Optical tweezers-based determination of Hc adhesion to Mφs.

Treatment of J774.16 Mφs with 10 mM m-*β*-CD (blue) results in a decreased during the adhesion kinetic, in comparison with systems using control Mφs (red). Antibody-treatment of Hc followed by interaction with control (green) or m-*β*-CD-treated (gray) Mφs enhances adhesion in comparison with systems where opsonization was not performed. The data shown are averages of results from 3 independent experiments. The error bars were determined as half the difference between the maximum and minimum values for each interval in 30 events performed in 3 distinct samples. The characteristic time (τ) required for adhesion is also shown.

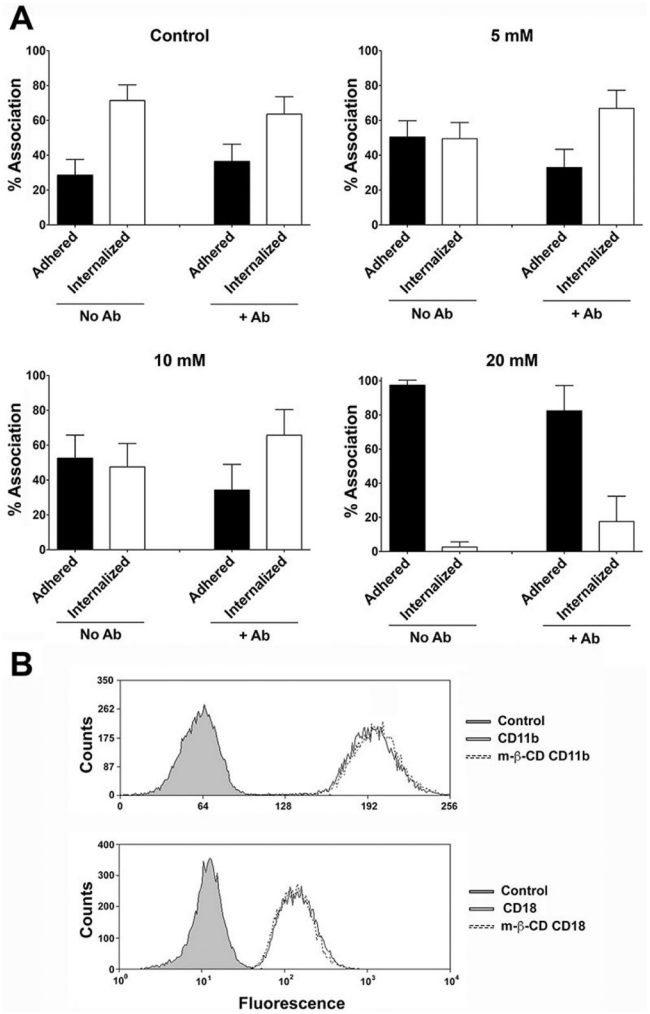

Figure 4 –. Disruption of membrane rafts by m-β-CD decreases adhesion and internalization of Hc yeasts.

(A) J774.16 Mφs were treated, or not with 5, 10 or 20 mM of m-β-CD and then incubated with non-opsonized (left panels) or anti-Hsp60 mAb opsonized (right panels) yeast previously labeled with NHS-Rho. After 45 minutes of interaction, Uvitex 2B was added to stain extracellular fungi. Percentages of adherent and internalized yeasts are only for Mφs associated with Hc. The effect on sterol depletion by m-β-CD treatment was overcome by yeast opsonization at concentrations of 5 and 10 mM, and partially reversed at 20 mM m-β-CD. (B) Mφs treated with 10 mM of m-β-CD were also labeled with anti-CD11b or CD18 to confirm the levels of CR3 on the cell surface and no changes were detected. The experiments were performed 3 different times with similar results. Statistical analyses of these data are shown in Supplementary Table 2.

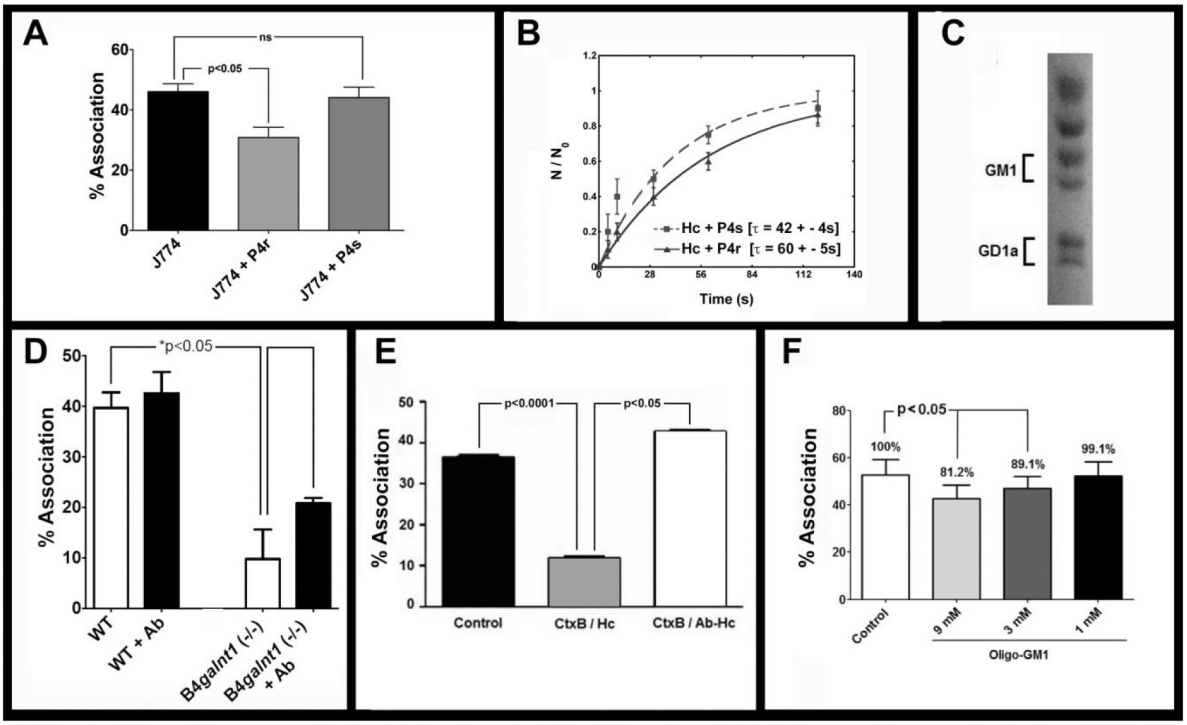

Figure 5 –. Inhibition of GSL synthesis and CtxB influences Hc- Mφ association.

(A) Inhibition of GSL expression decreases fungal association to J774.16 Mφ ($p<0.05$). Mφs treated with the CerGlcT inhibitor P4r (active isomer) for 3 days have a 70% inhibition of ganglioside expression whereas exposure to P4s (inactive isomer) had no effect (data not shown). Treated Mφs were incubated with GFP-Hc and the association index determined by FACS analysis. (B) Kinetics of Hc- Mφ adhesion measured by OT. Treatment of Mφs with P4r (Δ) results in decreased kinetics of adhesion compared with control systems (■). Characteristic time (τ) required for adhesion is shown. (C) TLC showing major gangliosides produced by J774 cells. GM1 and GD1a are indicated and were detected by immunoassays using specific mAbs (data not shown). (D) GFP-Hc yeast cells with or without opsonization with MAb 7B6 were incubated for 45 minutes with WT or *B4galnt1*$^{-/-}$ peritoneal Mφs. Samples were analyzed by flow cytometry. (E) Hc yeasts were incubated with J774.16 Mφs previously treated with CtxB (1μg/ml). Binding of CtxB to Mφ cell surface inhibited fungal association (CtxB/ Hc). Pre-treatment of yeasts with mAbs to HSP60 reversed the effect of CtxB (CtxB/Ab- Hc). Association percentage values normalized by the control are shown (above bars). (F) Hc yeast were co-incubated with oligo-GM1 and J774.16 Mφs. Inhibition of fungal association by oligo-GM1 was dose dependent. The experiments were performed at least twice with similar results.

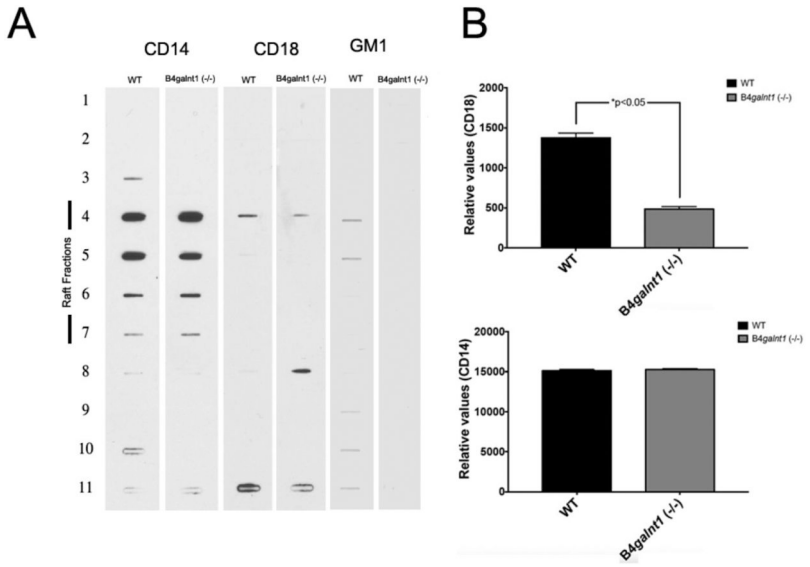

Figure 6 –. Complex gangliosides are required for correct CD18 recruitment to lipid microdomains.

(A) Lipid microdomains were isolated from WT and *B4galnt1*$^{-/-}$ mice Mφs. Fractions from sucrose gradients were probed with peroxidase-conjugated antibodies to CD14 or to CD18 (Becton Dickinson). Peroxidase-labeled CtxB (Sigma) was used to detect GM1. (B) Densitometric analysis of fractions corresponding to lipids microdomains was performed using ImageJ and the relative values from one experiment are presented. Experiments were performed three times with similar results (*p<0.05).

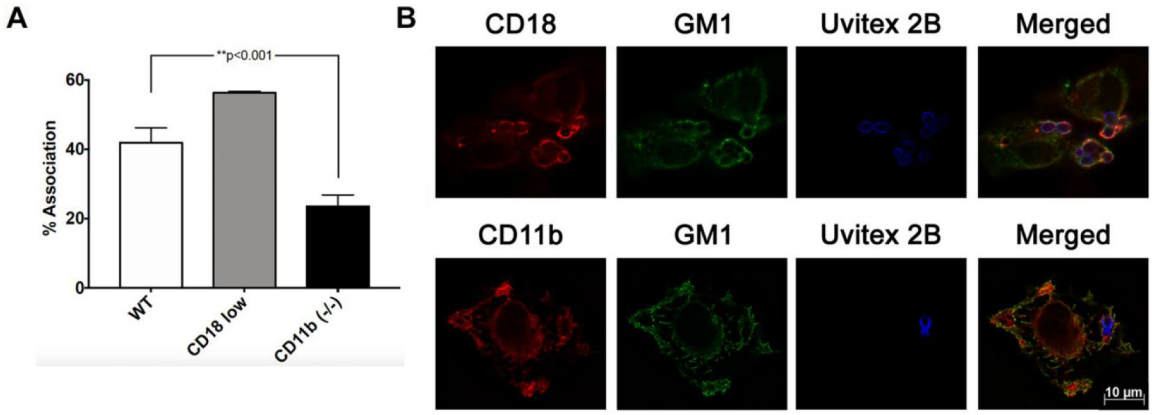

Figure 7 –. Participation of CD18 and CD11b during Hc- Mφs association.

(A) GFP-Hc yeast cells were incubated for 5 minutes with WT, *CD18*^{low} or *CD11b*$^{-/-}$ Mφs. The association levels were analyzed by flow cytometry (*p<0.001). (B) Bone marrow-derived murine Mφs were incubated with Uvitex 2B-labeled Hc for 15 minutes (moi 1:2), and the distribution of ganglioside GM1 (green), CD18 (red, upper panel) and CD11b (red, lower panel) were evaluated. The overlay images show the binding sites between Mφs and Hc by the colocalization of integrins and GM1. Bar, 10 μm.